Journal of Hazardous Materials 383 (2020) 121139

Contents lists available at ScienceDirect

Journal of Hazardous Materials

journal homepage: www.elsevier.com/locate/jhazmat

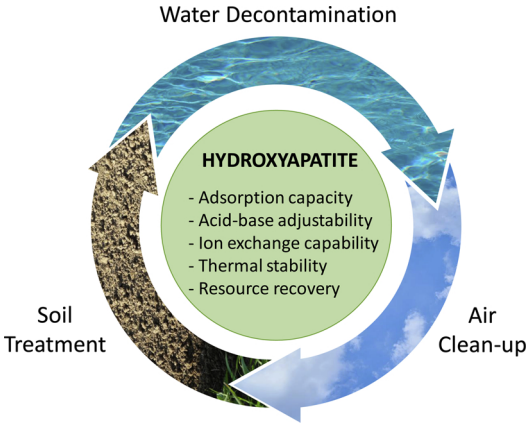
Review

Hydroxyapatite, a multifunctional material for air, water and soil pollution control: A review

Maya Ibrahim[a,b], Madona Labaki[b], Jean-Marc Giraudon[a], Jean-François Lamonier[a,*]

[a] Univ. Lille, CNRS, Centrale Lille, ENSCL, Univ. Artois, UMR 8181 – UCCS – Unité de Catalyse et Chimie du Solide, F-59000 Lille, France
[b] Lebanese University, Faculty of Sciences, Laboratory of Physical Chemistry of Materials LCPM/PR2N, Fanar, Lebanon

GRAPHICAL ABSTRACT



ARTICLE INFO

Editor: Deyi Hou

Keywords:
Hydroxyapatite
Pollution control
Adsorption
Catalysis
Resource recovery

ABSTRACT

Hydroxyapatite ($Ca_{10}(PO_4)_6(OH)_2$), a calcium phosphate biomaterial, is a very promising candidate for the treatment of air, water and soil pollution. Indeed, hydroxyapatite (Hap) can be extremely useful in the field of environmental management, due in one part to its particular structure and attractive properties, such as its great adsorption capacities, its acid-base adjustability, its ion-exchange capability and its good thermal stability. Moreover, Hap is able to constitute a valuable resource recovery route. The first part of this review will be dedicated towards presenting Hap's structure and defining properties that result in its viability as an environmental remediation material. The second will focus on its use as adsorbent for wastewater and soil treatment, while indicating the mechanisms involved in this remediation process. Finally, the last part will impart all findings on Hap's applications in the field of catalysis, whether it be as catalyst, as photocatalyst, or as active phase support. Hence, all of the above will have served in showcasing the benefits gained by employing hydroxyapatite in air, water and soil clean-up.

* Corresponding author at: University of Lille, UCCS C3 Building, 59650 Villeneuve d'Ascq, France.
E-mail address: jean-francois.lamonier@univ-lille.fr (J.-F. Lamonier).

https://doi.org/10.1016/j.jhazmat.2019.121139
Received 13 May 2019; Received in revised form 19 August 2019; Accepted 2 September 2019
Available online 04 September 2019
0304-3894/ © 2019 Elsevier B.V. All rights reserved.

1. Introduction

Calcium phosphates form a privileged class of biomaterials because of their good biocompatibility, their possibility of biodegradability and their possible bioreactivity. Depending on the Ca/P ratio, several families of calcium orthophosphates can be defined such as pyrophosphate (Ca/P = 1), octacalcium phosphate (Ca/P = 1.33), tricalcium phosphate (Ca/P = 1.5), hydroxyapatite (Ca/P = 1.67) and tetracalcium phosphate (Ca/P = 2).

Calcium phosphates are part of the apatites of the general formula $Me_{10}(XO_4)_6Y_2$ and which crystallize in the hexagonal system (space group: P6 3/m), where:

- (Me) represents a generally divalent cation (Ca^{2+}, Sr^{2+}, Ba^{2+}, Pb^{2+}, …) which can be replaced by monovalent cations (Na^+, Rb^+, Cs^+, K^+…), trivalent cations (Re^{3+} (rare earths), Al^{3+}, An^{3+} (actinides)…) and tetravalent cations (U^{4+}, Pu^{4+}, Th^{4+}…) ;
- (XO_4) is an anionic tetrahedron often trivalent such as PO_4^{3-}, AsO_4^{3-},VO_4^{3-} that can be substituted by a tetravalent group (SiO_4^{4-}, GeO_4^{4-}…) or even bivalent (SO_4^{2-}, CO_3^{2-}, HPO_4^{2-}…) ;
- Y is a site occupied by an anion that is often monovalent (F^-, OH^-, Cl^-…) and sometimes bivalent (O^{2-}, CO_3^{2-}…). Vacancies can also be found on the Y site.

The most common natural apatites are calcium phosphates of stoichiometry close to the general formula $Ca_{10}(PO_4)_6Y_2$ where Y = OH^-, F^-, Cl^-, where the fluoroapatite (Y = F^-) is the most thermodynamically stable.

Hydroxyapatite (Hap), whose general formula is $Ca_{10}(PO_4)_6(OH)_2$, is the primary mineral component of bone and teeth and the main factor responsible for their hardness and strength. This bio-inspired material is of great interest in many fields because of its remarkable structure and inherent properties. To cite a few, hydroxyapatite is considered to be very valuable for medical purposes in which it can be used as bone repairing material (Ioku, 2010; Sopyan et al., 2007; Mondal et al., 2016a) or as biocompatible coating for bioimplant materials that suffer from high degradation rate (Surmeneva et al., 2019, 2015). Moreover, Hap finds many applications in pharmaceutical industries where it is applied as a protein delivery media (Fu et al., 2013; Swain and Sarkar, 2013) and drug releasing agent (Palazzo et al., 2005; Weerasuriya et al., 2017; Son et al., 2011). Hap is also substantially used in chemical industries where chromatography on hydroxyapatite columns constitutes a powerful technique for separation of proteins and nucleic acids (Cummings et al., 2009; Tibbetts et al., 1973). On the other hand, regarding the pollution control field, which is the topic of this review, seeing as nowadays more and more efforts are being made towards environmental remediation industry (Condit et al., 2017), with the focus being shifted towards the development of new and improved ways of eliminating air (Wu et al., 2018), soil (Shaaban et al., 2018; Wlóka et al., 2019) and water (Holkar et al., 2016; Kumari and Saroha, 2018) pollution, the use of Hap can prove to be highly benefic for the removal of contaminants present in gas, liquid and solid phases.

We should mention that while a review covering the syntheses, structure and applications of this calcium phosphate in heterogeneous catalysis has been recently published (Fihri et al., 2017), there has not been yet a publication that explores this biomaterial in all three of air, water and soil decontamination processes, while also showing Hap's excellent performance even when obtained from natural sources.

Therefore, this present review will not go into the different methods and techniques of synthesizing hydroxyaptite, for the reason that this has already been largely discussed in previous reviews (Fihri et al., 2017; Haider et al., 2017; Prakasam et al., 2015). It will instead report both old and recent works that have been done on the usage of hydroxyapatite, with the purpose of controlling and reducing the risks posed by the presence of hazardous materials in the environment. In fact, employing hydroxyapatite in air, water and soil clean-up will not only constitute a sustainable, safe and clean method for pollutants' removal from contaminated sites, but also make up for a valuable resource recovery route, since Hap can be successfully obtained from biological sources, such as mineral rocks, plants…, and more importantly from waste, among which essentially figure animal bones (fish bones, chicken bone …), as well as biogenic products (eggshells, mussel shells …).

To put it concisely, this review will begin, firstly, by providing an insight into the structure and defining properties of hydroxyapatite in order to better understand its significant value and vital contribution to the field of environmental management. Secondly, a presentation of the use of hydroxyapatite as adsorbent for wastewater and soil treatment will give adequate knowledge of the process involved in such remediation methods, thus, emphasizing the crucial role played by the apatitic compound on the procedure's outcome in regards to viability and efficiency. Finally, an extensive survey of the various applications of Hap in catalysis, first as a catalyst, second as a photocatalyst, and thirdly as the active phase support, will allow highlighting the diversified and numerous practical applications of this calcium phosphate complex in catalytic reactions, showcasing its contribution in attaining better catalytic performances.

2. Hydroxyapatite material

2.1. Structure

Hap crystallizes in the hexagonal system (P63/m space group) and the approximate lattice parameters are: a = 9.37 Å and c = 6.88 Å. It is important to note that there are two crystallographically different Ca atoms. Hence, the general formula of the Hap can be rewritten as $Ca(I)_4Ca(II)_6(PO_4)_6(OH)_2$. In fact, as can be seen in Fig. 1, the framework of hydroxyapatite can be described as a compact assemblage of tetrahedral PO_4 groups where each PO_4 tetrahedron is shared by one column, and delimit two types of unconnected channels. The first channel has a diameter of 2.5 Å and is bordered by Ca^{2+} ions (denoted Ca (I)). The second type, which plays an important role in the acid-base and electrical properties of apatite-type solids, has a diameter of around 3.5 Å, is bordered by triangular Ca^{2+} ions (denoted Ca(II)), and hosts the OH groups along the c- axis in order to balance the positive charge of the matrix (Elliott et al., 2002; Elliot, 1994; Pasteris, 2012).

The aforementioned Hap allows large variations in compositions, and, as a matter of fact, can be a highly non-stoichiometric solid. Stoichiometric Hap (Hap-S) has the chemical formula $Ca_{10}(PO_4)_6(OH)_2$ where the ratio Ca/P is of 1.67. Calcium deficient Hap (Hap-D) has a Ca/P ratio less than 1.67 and its chemical formula is $Ca_{10-x}(HPO_4)_x(PO_4)_{6-x}(OH)_{2-x}$ with $0 < x < 1$, and finally carbonate-rich

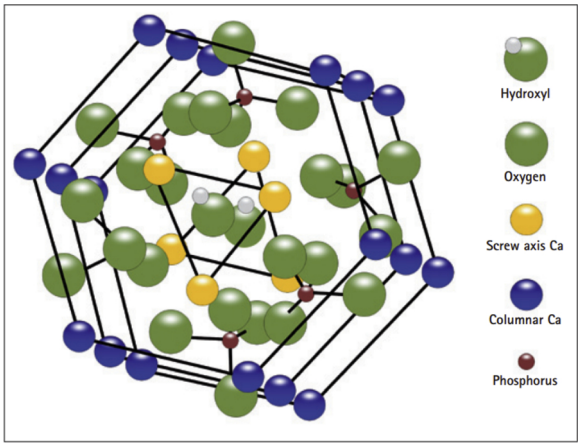


Fig. 1. Illustration of the structure of hydroxyapatite. From reference (Brunton et al., 2013).

hydroxyapatite (Hap-E) with the chemical formula $Ca_{10-x}(PO_4)_{6-x}(CO_3)_x(OH)_{2-x}$, or $Ca_{10-y}Na_y[(PO_4)_{6-y}(CO_3)_y][(OH)_{2-2x}(CO_3)_x]$ in case sodium is present, has a Ca/P ratio higher than 1.67 (Chlala et al., 2016a; Nishikawa et al., 2012).

Furthermore, Hap is poorly soluble in water and insoluble in alkaline solutions. It is, however, soluble in acids because both PO_4^{3-} and OH^- react with H^+ (Meza et al., 2011; Li et al., 2016):

$$Ca_{10}(PO_4)_6(OH)_2 + 14\ H^+ \rightarrow 10\ Ca^{2+} + 6\ H_2PO_4^- + 2\ H_2O \quad (1)$$

This apatitic biomaterial has attracted much attention in numerous applications due to its varied useful properties, which we will strive to clearly outline in the upcoming part.

2.2. Properties

2.2.1. Adsorption capacities

The adsorption properties of a material are of significance when exploring environmental remediation technologies and the catalytic activity of heterogeneous surfaces. Indeed, on the one hand, the adsorbent material can contribute to the removal of pollutants by retaining them on its surface, and on the other hand, it can facilitate the catalytic process seeing as an adsorption followed by an activation of the reactants on the surface of catalysts constitutes a critical step in catalytic reactions.

It is well-known that hydroxyapatite possesses great adsorption capacities, a property which favored its use in chromatographic columns for the separation of proteins, nucleic acids and viruses (Cummings et al., 2009; Bernardi, 1973; Tiselius et al., 1956; Bernardi, 1971a; Kadoya, 1990; Itagaki et al., 1993; Bernardi, 1971b; Watanabe et al., 1999; Kawasaki et al., 1985).

Indeed, literature reports Hap as having two distinct binding sites, C and P sites, present on its surface. C sites, which consists of calcium ions are positively charged, and preferentially adsorb acid molecules, while P sites which consists of phosphate groups are negatively charged, and preferentially adsorb basic molecules (Kandori et al., 2009; Yin et al., 2002).

In addition, hydroxyapatite presents two types of crystal planes, each displaying its characteristic atomic arrangement. In fact, whereas the a(b)-planes expose, primarily, positively charged Ca ions, the c-planes expose negatively charged phosphate and hydroxyl groups. This fact encouraged researchers to examine the possibility of obtaining a selective adsorption behavior, depending on the orientation of prepared Hap material. The work of Zhuang et al. (Zhuang and Aizawa, 2013), demonstrated the validity of this hypothesis, since the study of the adsorption of bovine serum albumin (BSA), an acidic protein, and lysozyme (LSZ), a basic protein, onto synthesized Hap particles with preferred orientation to the c- and a(b)-axes, resulted in a high specificity for the adsorption of BSA and LSZ, on a- and c-oriented hydroxyapatite, respectively.

Furthermore, an investigation conducted by Kandori et al. (2009) on the influence of heat treatment on the protein sorption properties of Hap, revealed an enhanced adsorption performance of acidic and basic proteins that comes with the sintering of this material, as can be clearly seen in Fig. 2. This was ascribed to an increase of calcium and phosphate ions in the media (Fig. 2), generated by the formation of β-tricalcium phosphate, $\beta\text{-}Ca_3(PO_4)_2$. As a matter of fact, seeing as these ions are considered to be binding sites between non-neutral proteins (such as BSA and LSZ) and Hap surfaces, it could be easily understood how a rise of their amount could lead to an enhanced adsorption behavior (contrarily to what is noted in the case of neutral myoglobin MGB).

Moreover, it is really important to realize that based on the properties of the adsorbate, it is possible to improve Hap's adsorption performances by simply adjusting certain parameters to better fit the required application. For example, a most influential parameter that should be taken into account when synthesizing Hap in the aim of utilizing its adsorption properties, is the molar ratio Ca/P. A variation of this ratio could either enhance or worsen Hap's adsorption efficiency, depending on the acido-basicity nature of the adsorbate. Since an increase of the molar ratio Ca/P would be beneficial in the case of an acidic molecule's adsorption, yet disadvantageous in the adsorption of a basic compound (Swain and Sarkar, 2013).

2.2.2. Acid-base adjustability

In the field of heterogeneous catalysis, the acid-base properties of solid catalysts are known to play a key-role in their catalytic performance; the number and strength of the acid/base sites being crucial factors driving the activity and selectivity of many catalytic reactions, not only in acid-base transformations but also in reduction and oxidation reactions.

Hap has the rare property of containing both acid and basic sites in its inherent structure. This property is strongly correlated to the Ca/P atomic ratio in the calcium phosphate compound. Thus, it can be modified accordingly in order to obtain the desired acidic and/or basic function (Silvester et al., 2014; Lamonier et al., 2011).

In fact, the higher the Ca/P ratio is, the lower the acid site density and the higher the basic site density is. Indeed, at Ca/P ratio of 1.50, Hap acts as an acid catalyst. However, when Ca/P = 1.67, hydroxyapatite demonstrates basic behavior; and so, when the Ca/P ratio is between 1.50 and 1.67, Hap develops both acidic and basic attributes. Therefore, deficient Haps are considered to be acid solids, and the nearer we draw to the stoichiometric apatite (predominantly basic) the more basic the solids are. This was verified by various authors through different Hap catalyzed reactions. Studies of the reactivity of ethanol over hydroxyapatite revealed an association between the Ca/P ratio of Hap catalysts and selectivity to certain products (Tsuchida et al., 2008; Silvester et al., 2015). Ethylene was the main product when the Ca/P ratio of the catalysts was low (Ca/P ratio of 1.50), the acid solid catalyzing predominantly the dehydration reaction, whereas the best selectivity for 1,3-butadiene was observed for Ca/P ratio of 1.62, where the apatitic structure displayed a relative balance of acid and basic sites. On the other hand, acetaldehyde, the dehydrogenation product of ethanol, was mainly produced over Hap catalysts with high Ca/P ratios. Other reactions were also examined and exhibited many similarities to the one described previously (Silvester et al., 2014; Lamonier et al., 2011; Kibby and Hall, 1973).

In order to better understand the correlation between the Ca/P ratio and the acid-base properties, it is important to note that the acidity of Hap derives from two types of acid sites: Brönsted acid sites and Lewis acid sites, illustrated by Silvester et al. (2014) in Fig. 3. HPO_4^{2-} species act as the former while Ca^{2+} or OH^- vacancies result in the latter. This explains why calcium-deficient apatite HapD has a higher number of acid sites. This is due to the contribution from HPO_4^{2-} groups, abundantly present in this type of apatite, or OH^- vacancies. Hence, HapD is more acid and contains more Brönsted acid sites, when compared to stoichiometric and calcium-rich hydroxyapatite (Silvester et al., 2014; Tsuchida et al., 2008; Diallo-Garcia et al., 2014).

What is more, regarding water decontamination processes which involve, among other things, metal trapping on a suitable adsorbent material, surface properties such as surface acido-basicity of the Hap matrix can play an important role in determining the predominance of a particular metal immobilization mechanism. Hence, it was useful to not only measure the acid-base properties of hydroxyapatite in air (Silvester et al., 2014) but also in water (Ferri et al., 2019), since it would serve to evaluate the characteristics of Hap's surface under real working conditions (decontamination of metal-polluted waters). Surface acid and basic sites of hydroxyapatite solid can be measured in gas phase by Thermo-Programmed Desorption of NH_3 (TPD-NH_3) and of CO_2 (TPD-CO_2), respectively, whereas in liquid phase, they can be assessed by titration with solutions of 2-phenylethylamine (PEA) and benzoic acid (BA), respectively. Interestingly, researchers found that even though

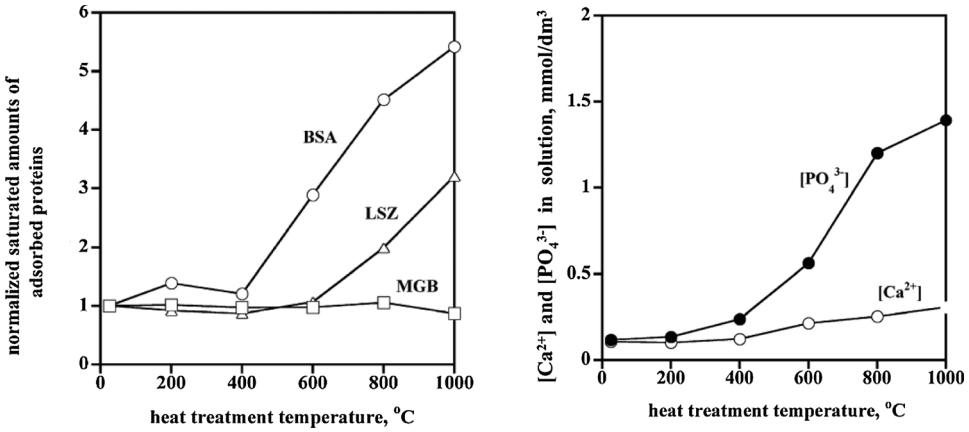


Fig. 2. (Left) Plots of normalized saturated amounts of adsorbed proteins as a function of heat treatment temperature. (Right) Concentrations of calcium and phosphate ions in the supernatant dissolved from the Hap particles after treatment at various temperatures. Reprinted with permission from (Kandori et al., 2009). Copyright 2019 American Chemical Society.

stoichiometric Hap is a basic rather than an acidic material, in water it only exhibits acidic property because Hap's basic sites are too weak to provide it with lively basicity (Ferri et al., 2019).

An additional noteworthy point to consider is the possibility of tuning the surface's acido-basicity by cationic and anionic substitutions (Silvester et al., 2014; Lamonier et al., 2011; Oh et al., 2016; Resende et al., 2006; Oh et al., 2017). For example, the addition of sodium ions causes a slight increase in the basicity of hydroxyapatite materials (Lamonier et al., 2011), whereas acidity is largely enhanced by replacing OH^- by CO_3^{2-} anions (Resende et al., 2006). As a matter of fact, this remarkable substitution aptitude will be further discussed below.

2.2.3. *Ion-exchange capability*

Ion-exchange is one of the most common and effective treatment methods used in pollution control. Through the removal of hazardous ionic impurities and the recovery of toxic and valuable metals from hostile surroundings (nuclear waste), ion-exchange materials play an increasing role in waste minimization and management.

This is why it is important to mention that the apatite lattice is very flexible. Thus, it is very tolerant of substitutions and allows the presence of defects and vacancies. The substitution can occur in either the cationic or the anionic sites. When it comes to the first one, calcium ions can be replaced by different metal ions such as transition metals (Tounsi et al., 2011; Matsunaga et al., 2010; Zhu et al., 2006; Veselinović et al., 2010; Wakamura et al., 2000) (Cu^{2+}, Mn^{2+}, Ni^{2+}, Zn^{2+}, Cd^{2+}, Co^{2+}…), alkaline earth metals (Zhu et al., 2006; Laurencin et al., 2011) (Mg^{2+}, Sr^{2+}, Ba^{2+}…) and many other cations (Zhu et al., 2006; Kandori et al., 2010) (Pb^{2+}, Al^{3+}, La^{3+}…).

However, the determination of the occupation site remains delicate. Indeed, as explained above, there are two types of nonequivalent sites when it comes to calcium ions denoted Ca(I) and Ca(II). Discerning an ion's preferential position requires better understanding of the parameters that govern a cation's affinity to a specific site. According to Zhu et al. (2006), the preferential occupancy of metal ions can be explained mainly by ionic radius and electronegativity of the metal ions, Ca(II) sites being preferentially occupied by cations with bigger ionic radius or electronegativity than Ca^{2+}. Hence, these authors were able to illustrate the reason for all of Cd^{2+} (similar ionic radius but bigger electronegativity), Sr^{2+} (similar electronegativity but bigger ionic radius) and Pb^{2+} ions (bigger ionic radius and electronegativity) preferential occupancy of the Ca(II) sites in the apatite structure. These findings were also verified by other researchers (Veselinović et al., 2010; Opre et al., 2005; Opre, 2007) who confirmed larger ions' stronger preference towards Ca(II) site and smaller ones towards the Ca(I) site and corroborated electronegativity's impact on the distribution of the cations between the two positions.

Moreover, it is important to discuss the factors that influence the facility of the exchange process. Following the results obtained from their work, Wakamura et al. (2000) were able to establish that the ion-exchange with Ca^{2+} seems to depend more on the cations' charge density than on its ionic radius, an ion with larger charge density displacing more easily calcium ions than an ion of a similar ionic size.

As for anionic substitutions, they involve either OH^- or PO_4^{3-} ions or both. OH^- can be replaced by F^- (Veiderma et al., 2005; Hidouri et al., 2003; Silva et al., 2008; Prener, 1967; Rulis et al., 2004), Cl^- (Prener, 1967; Rulis et al., 2004; Elliott and Young, 1967), Br^- (Rulis et al., 2004; Duff, 1972), O^{2-} (Trombe and Montel, 1978) or CO_3^{2-} (Lafon et al., 2008; Barralet et al., 1998) and PO_4^{3-} by HPO_4^{2-}

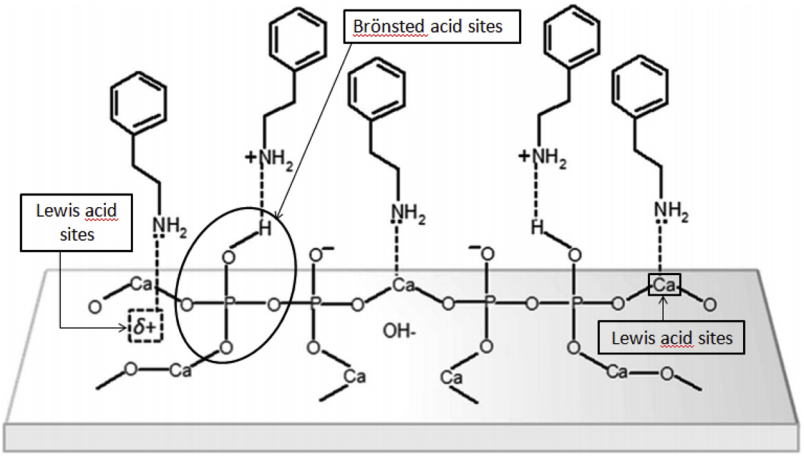


Fig. 3. Model of 2-phenylethylamine (used as a probe molecule) adsorption over Lewis and Brönsted acid sites on the surface of apatites [(δ+) = OH^- vacancies]. Adapted from reference (Silvester et al., 2014) - Published by The Royal Society of Chemistry.

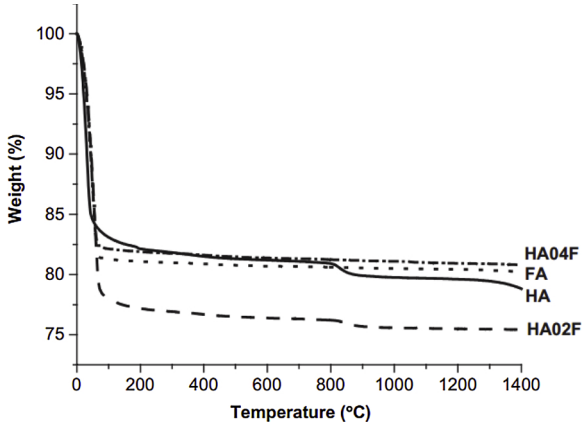


Fig. 4. TGA (thermogravimetric analysis) data of HA (hydroxyapatite), FHA (fluorine-substituted hydroxyapatite: HA04 F and HA02 F) and FA (fluorapatite) powders heated to 1400 °C in dry air. From reference (Chen and Miao, 2005).

(Ishikawa et al., 1993), AsO_4^{3-} (Dungkaew et al., 2012; Mahapatra et al., 1989), VO_4^{3-} (Boechat et al., 2000; Sugiyama et al., 2006), SO_4^{2-} (Veiderma et al., 2005), SiO_4^{4-} (Gibson et al., 1999) or CO_3^{2-} (Veiderma et al., 2005; Lafon et al., 2008; Barralet et al., 1998). In the case of carboapatites, the replacement with carbonate ions can occur at two different sites as can be seen in the following formula $Ca_{10-x/2}[(PO_4)_{6-x}(CO_3)_x][(OH)_{2-2y}(CO_3)_y]$. The substitution of hydroxyl and phosphate ions by carbonate, leads to A and B type carbonated hydroxyapatite respectively (Suetsugu et al., 2000; Fleet and Liu, 2007). Some studies went even further and identified three structural locations for the carbonate ions by differentiating between two types of channel positions: type A1 (apatite channel, oriented with two oxygen atoms close to the c-axis) and type A2 (stuffed channel position) (Fleet et al., 2004). It was also shown that the location site of CO_3^{2-} is strongly dependent on the synthesis method used to prepare carboapatites. In fact, type A apatite can be obtained by synthesizing the material at high temperature (~900 °C) or by heating the hydroxyapatite in a CO_2 atmosphere at temperatures of 900–1000 °C for 15–144 h, or also, by soaking stoichiometric Hap in an aqueous solution saturated in carbon dioxide for up to 2 months. Conversely, B type carbonated hydroxyapatite results from low temperatures (~400 °C) synthesis by precipitation at elevated pH (Resende et al., 2006; Gibson and Bonfield, 2002).

In short, Hap's ion exchange capacity has been widely explored in numerous works, in order to incorporate certain entities into the apatite structure (Tounsi et al., 2011; Kandori et al., 2010; Opre et al., 2005; Liu et al., 2010; Jemal et al., 2012; Khachani et al., 2010; Riad and Mikhail, 2012; Sugiyama et al., 1998; Matsuda et al., 2005; Li et al., 2010; Masuyama et al., 2011). These added substances can alter the physicochemical properties of the material and its effectiveness, thus, inducing the enhancement of Hap's catalytic activity and performance all while maintaining its overall structure.

2.2.4. Thermal stability

Thermal stability is one of the determining factors of a catalyst lifetime, seeing as thermal sintering is a major cause of irreversible catalyst deactivation. Therefore, when choosing a material to be utilized in environmental remediation processes, its thermal stability is regarded as an important consideration.

Hence, it comes as a significant value that another primary characteristic of hydroxyapatite is its good thermal and chemical stability. In fact, it is one of the major reasons that make it an attractive material choice and an excellent candidate for biomedical applications (Liu and Peng, 2015; Green, 1998; Epinette and Manley, 2003; Fu et al., 2016; Yoruç et al., 2012). Hap maintains its stability at a wide pH and temperature range. However, it is known to start to decompose into other phases such as tricalcium phosphate (TCP; $Ca_3(PO_4)_2$) at temperatures higher than 800 °C (El Idrissi et al., 2014; Eslami et al., 2008; Nilen and Richter, 2008; Ribeiro Alves et al., 2016):

$$Ca_{10}(PO_4)_6(OH)_2 \rightarrow 3\ \beta\text{–}\ Ca_3(PO_4)_2\ +\ CaO +\ H_2O \quad (2)$$

Nevertheless, there are certain factors influencing Hap's stability and upon which the latter is intrinsically dependent. Indeed, among these factors figures the apatite's stoichiometry as well as the synthesis conditions. It has actually been reported that stoichiometry plays a key role in apatite's stability, non-stoichiometric hydroxyapatites (Ca/P ratios different from 1.67) being less thermally stable than stoichiometric ones. In fact, research has shown that Hap with Ca/P = 1.68 can reach temperatures up to 1450 °C without decomposing over a period of 3 h, consequently making stoichiometry a most looked-for criteria owing to the stability it provides at high temperatures (Orlovskii et al., 2002; Barbucci, 2007; Malina et al., 2013). Furthermore, Fang et al. (1994) found an optimum thermal stability (up to 1370 °C) for Hap samples prepared by hydrothermal method, whereas Hap synthesized by hydrolysis of brushite started to decompose at about 700 °C. In a different study, calcium phosphates which were synthesized by a modified wet chemical precipitation route where calcium hydroxide was homogenized with planetary mill resulted in a highly thermally stable (up to 1300 °C) hydroxyapatite, hence, demonstrating the effect of synthesis parameters on the apatite's stability (Salma et al., 2010).

Moreover, the incorporation of ions into the hydroxyapatite structure can also affect the crystal lattice properties, therefore enhancing or diminishing Hap's thermal and chemical stability. For example, the introduction of fluoride ions into the apatite lattice ($Ca_{10}(PO_4)_6(OH)_{2-2x}F_{2x}$) with varying amounts (x = 0, 0.2, 0.4, and 1.0, in HA, HA02 F, HA04 F and FA, respectively) improves the thermal and chemical stability when x > 0.4 by hindering the decomposition process, as evidenced by Fig. 4, and by ameliorating Hap's corrosion resistance (Cai et al., 2011; Kanchana and Sekar, 2010; Karamian et al., 2016; Kapoor et al., 2016; Nasiri-Tabrizi et al., 2012; Chen and Miao, 2005; Wang et al., 2007; Zhang et al., 2006; Lee et al., 2005a; Kim et al., 2004; Zhang, 2013; Park and Lakes, 2007). Other substitutions can, on the contrary, reduce the material's stability by increasing its solubility such as strontium, magnesium, manganese and carbonate substitutions (Ungureanu et al., 2011; Kuśnieruk et al., 2016; Zilm et al., 2015).

2.3. Factors that make Hap an environment-friendly material

Hydroxyapatite is considered to be an environment-friendly material for many reasons, among which figure its non-toxicity and biocompatibility. This latter, combined with its excellent osteoconductive property, have led to Hap playing a vital role in clinical applications such as drug delivery (Mondal et al., 2018), bone tissue regeneration (Denry and Kuhn, 2016), as well as various other fields which help in reducing the environmental pollution. In fact, we will discuss, in detail, the use of hydroxyapatite in these ecologically related applications in the following section.

However now, we will focus more on another aspect that makes this calcium phosphate compound particularly attractive from an environmental point of view, besides its intrinsic properties and its environmental applications. It is actually its capacity to be derived from natural sources, and more precisely from waste. Indeed, Hap has been successfully obtained from animal waste such as fish bones (Boutinguiza et al., 2012; Piccirillo et al., 2014; Pal et al., 2017), chicken bone (Rajesh et al., 2012), fish scales (Piccirillo et al., 2014; Muhammad et al., 2016; Mondal et al., 2016b; Pon-On et al., 2016; Chai and Tagaya, 2018), eggshells (Abdulrahman et al., 2014; Bardhan et al., 2011; Baba et al., 2013), and mussel shells (Jones et al., 2011), all of which were found to constitute important bioresources for hydroxyapatite production. Nonetheless, it is important to mention that hydroxyapatite derived from natural sources differ from synthetic Hap in

terms of lower purity, higher degree of substitution and deficiency, lower specific surface area value (4.49 $m^2.g^{-1}$ for natural phosphates (Kaluđerović Radoičić and Raičević, 2008) while that of synthetic Hap can attain 100 $m^2.g^{-1}$ and more) and consequently, poorer sorption capacities (Kaluđerović Radoičić and Raičević, 2008; Joschek et al., 2000; El Asri et al., 2010; Admassu and Breese, 1999; Haberko et al., 2006; Ooi et al., 2007; Leventouri, 2006; Zhou et al., 2017). Indeed, bio-sources of Hap contain small amounts of inorganic compounds other than Hap, such as $Ca_4O(PO_4)_2$, $NaCaPO_4$, $Ca_3(PO_4)_2$, CaO, and MgO. In addition, through Hap's substitution ability, natural apatite contains some fluoride or chloride in place of hydroxide and some metal ions (aluminum, iron, copper, zinc…) in place of Ca^{2+}. Finally, organic matters are also present within natural apatitic materials. All of these alterations in the compound's purity and therefore in the obtained Ca/P value (Kaluđerović Radoičić and Raičević, 2008; Haberko et al., 2006), can have a direct influence on the efficiency of hydroxyapatite used in environmental remediation applications. This is why, a pre-treatment of naturally derived Hap is usually conducted before its use, in order to eliminate remaining organic matter and attain a pure hydroxyapatite phase, which would result in a Hap material with comparable properties and efficiency as synthetic hydroxyapatite.

What is important to understand is that this generation of Hap from waste does not only offer economic benefits since it relies on the use of cheap, natural and undesirable materials, but also, contributes in achieving a sustainable development by being an active part in the global waste management process. In other words, solids which would have accumulated, creating thus a pollution source, endangering human, animal and vegetation's health, are in this way being utilized for the production of very sought-out product.

All of the above cited factors lead to hydroxyapatite being branded an environment-friendly material. As mentioned before, we will present thoroughly, in the remaining part of this review, the different environmentally related applications of Hap.

3. Hap as adsorbent for wastewater and soil treatment

3.1. Metals removal

Heavy metals are recognized for being a serious threat to plants, animals and even humans because of their bioaccumulation, non biodegradable property and toxicity even at low concentrations. Therefore, the removal of heavy metal ions from aqueous solutions and contaminated grounds has become an environmental necessity, requiring the setting up of treatment technologies and decontamination processes. Among the available techniques, sorption proves to be a very efficient, economical and simple method to perform. Hydroxyapatite makes for a perfect choice of sorbent for long-term containment of pollutants seeing as this mineral material possesses the following excellent properties: non-toxic, inexpensive and readily available, high adsorption capacity, low water solubility, and high stability under reducing and oxidizing conditions.

Indeed, Hap turned out to be very efficient in immobilizing metals such as: Cr, Pb, Cd, Ni, Zn, Al, Cu, Fe, Co, Mn, and Fe (Ferri et al., 2019; Flores-Cano et al., 2016; Mobasherpour et al., 2012; Hadioui et al., 2008; Ma et al., 1993; Reichert and Binner, 1996; Mousa et al., 2016; Feng et al., 2010; Ma et al., 1994a, ; Chen et al., 1997a, 2007; Chen et al., 1997b; Srinivasan et al., 2006; Xu et al., 1994; Prasad et al., 2008; del Rıo et al., 2004; Og and Fa, 2018; Corami et al., 2008; Campisi et al., 2018; Mobasherpour et al., 2011; Smičiklas et al., 2000; Lee et al., 2005b), as well as many others. Nonetheless, it is worth mentioning that in the work of Mobasherpour et al. (2012) hydroxyapatite exhibited preferential adsorption of some cations over others, because of its greater affinity to said cations. In fact, the removal capacity of Pb^{2+}, Cd^{2+} and Ni^{2+} increased in the following order: $Pb^{2+} > Cd^{2+} > Ni^{2+}$. Several hypotheses were given to explain this tendency of cation preference. One was the difference in the acidity strength among these ions. Pb^{2+} is considered a borderline hard Lewis acid, while Cd^{2+} and Ni^{2+} are classified among the soft Lewis acids. Seeing as the phosphate and hydroxyl groups in hydroxyapatite are hard Lewis bases, this would explain this material's higher affinity for lead cations. Another reason for the preferential adsorption of Pb^{2+} on Hap would be its higher electronegativity, compared to that of Cd and Ni, a factor which would facilitate surface complexation reactions. Besides, based on LeGeros and Legeros (1984), cations with ionic radii bigger than Ca^{2+} (0.099 nm) are more likely to be incorporated into Hap's structure than cations with similar or smaller ionic radii. Since the ionic radii of Pb^{2+}, Cd^{2+} and Ni^{2+} are, respectively, 0.118 nm, 0.097 nm and 0.072 nm, it is more than logical to obtain the sequence of preferential adsorption cited above.

In addition, one important factor which may influence Hap's sorption capacities is its degree of crystallinity. A correlation between the crystallinity of hydroxyapatite and its ion adsorption behaviour was actually found in a study conducted by Stötzel et al. (2009). These authors stated that a decrease of Hap's crystallinity (crystallinity = 95, 65, 22 and 0%, in the case of powders calcined at 1000 °C, calcined at 700 °C, mesocrystalline and nanocrystalline powders, respectively), leading to a growth of its specific surface area, is beneficial to this material's sorption properties and its ability to remove heavy metal ions, as evidenced by Fig. 5. Furthermore, this work revealed that nanocrystalline hydroxyapatite powder outperforms activated carbon in the removal of both divalent metals examined in their study (Pb^{2+} and Zn^{2+}) by nearly one-order of magnitude, all of which demonstrates the attractiveness of this apatitic sorbent as a heavy metal immobilizer.

Another element able to affect hydroxyapatite's performance as an adsorbent material is the alteration of its Ca/P molar ratio, which would cause a modification of its surface properties, such as the typology and location of carbonate species present in Hap. Indeed, depending on the nature of the polluting metal this could be a determining point of the metal removal efficiency of the Hap solid (Campisi et al., 2018).

Moreover, when compared to other phosphate containing materials (phosphate rock, triple-superphosphate, and diammonium phosphate), the activity of Hap surpassed that of the rest of these mineral solids in its aptitude to lessen the bioavailability of studied metals (cadmium, lead, and zinc) in an artificially metal-contaminated soil (Chen et al., 2007). We should mention that even when prepared from waste materials such as phosphogypsum waste (Mousa et al., 2016) and waste oyster shells (Lee et al., 2005b), hydroxyapatite proved to be an economical and efficient sorbent for heavy metals encountered in wastewater.

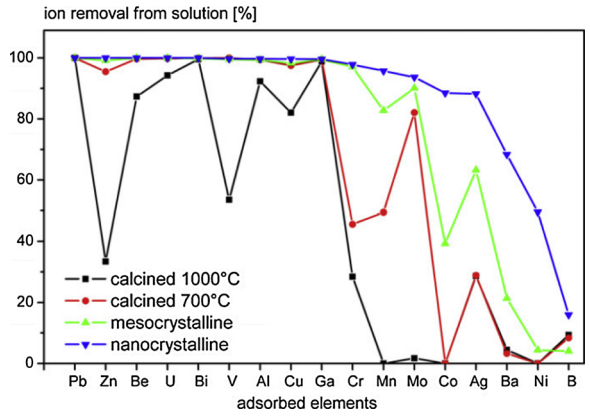


Fig. 5. Comparison of the ion adsorption potential of HA powders with different crystallinities. The powders were immersed in a multi-component ion solution (1000 mg/L Ca, 100 mg/L Be, B, Fe, Zn, As, Se and 10 mg/L Li, Na, Mg, Al, K, V, Cr, Mn, Co, Ni, Cu, Zn, Ga, Sr, Mo, Rb, Ag, Cd, Te, Ba, Tl, Bi, Pb, U; this solution being diluted with double distilled water to concentrations of 100–1000 ppb) for 10 min. From reference (Stötzel et al., 2009).

3.1.1. Two mechanisms

An essential subject of many discussions concerning the use of Hap as sorbent material, was the manner in which hydroxyapatite would remove these unwanted metals. In the following section, we will detail two of the most significant mechanisms of metal adsorption, knowing that there are others less commonly mentioned (surface complexation, solid diffusion…).

3.1.1.1. Dissolution-precipitation. In this type of mechanism, a dissolution of the hydroxyapatite occurs, supplying the media with phosphate ions which are capable of precipitating other surrounding metal cations (Me), creating thus a new metal phosphate crystal with an apatitic structure. This process can be portrayed by these two equations (Stötzel et al., 2009):

$$Ca_{10}(PO_4)_6(OH)_2 + 14\ H^+ \rightarrow 10\ Ca^{2+} + 6\ H_2PO_4^- + 2\ H_2O \quad (3)$$

$$Me^{2+} + 6\ H_2PO_4^- + 2\ H_2O \rightarrow Me_{10}(PO_4)_6(OH)_2 + 14\ H^+ \quad (4)$$

According to literature, among the various heavy metals which sorption mechanism was studied in the presence of a hydroxyapatite solid, one stands out as being primarily immobilized through a dissolution-precipitation mechanism, and it is none other than lead (Ma et al., 1993, 1994a; Ma et al., 1994b; Chen et al., 1997b; Srinivasan et al., 2006). Indeed, it has been proven throughout several studies that the removal process of Pb ions occurs mainly by the dissolution of hydroxyapatite and the formation of a lead-phosphate material. Though, depending on the anions present in the solution, the nature of the new crystal formed can vary, without affecting, however, the Hap's lead removal ability. Indeed, based on the work of Ma et al. (1994b), hydroxyapatite was able to immobilize Pb^{2+} cations in the presence of NO_3^-, Cl^-, F^-, SO_4^{2-}, and CO_3^{2-} anions, establishing once and for all its great potential for being used in removing Pb^{2+} from contaminated wastes, where such anions are bound to be present. The only variation noted when adding these anions to the media was the nature of lead precipitate obtained. While hydroxypyromorphite [$Pb_5(PO_4)_3OH$] was formed in the presence of NO_3^-, SO_4^{2-}, and CO_3^{2-}, chloropyromorphite [$Pb_5(PO_4)_3Cl$] and fluoropyromorphite [$Pb_5(PO_4)_3F$] were formed in the presence of Cl^- and F^-, respectively.

3.1.1.2. Ion exchange. A different but equally common sorption mechanism is ion exchange, in which divalent metal ions (Me) substitute calcium ions present in the Hap lattice through a process represented by the following equation (Stötzel et al., 2009):

$$Ca_{10}(PO_4)_6(OH)_2 + x\ Me^{2+} \rightarrow Ca_{10-x}Me_x(PO_4)_6(OH)_2 + x\ Ca^{2+} \quad (5)$$

When it comes to some metal ions such as cadmium (Srinivasan et al., 2006; del Rıo et al., 2004), or nickel (Mobasherpour et al., 2011) an ion exchange with Hap is rapid and more favorable to take place than a dissolution-precipitation process.

Interestingly enough, an investigation of the influence of the pH of the solution on the Hap uptake of the heavy metals present in the solution, could give an indirect indication on the sorption mechanism at play when it comes to each cation studied. For while a dissolution-precipitation process is facilitated in an acidic environment, an ion-exchange one is enabled in alkaline conditions. Indeed, Vila et al. (2011), found that the efficiency of lead removal by Hap, which is conducted by dissolution-precipitation mechanism, was higher at low pH and decreased with increasing alkalinity. This is easily explained by the change in hydroxyapatite solubility with variable pH (Hap solubility decreases with increasing pH) which when lessened limits the amount of phosphate ions dissolved and therefore the amount available for the Pb precipitation process. On the other hand, Chen et al. (1997a), who examined the effects of pH on heavy metal removal by mineral apatite, discovered that a low pH could be detrimental for the removal of cadmium and zinc from the solution, seeing as the sorption of theses cations on Hap was mainly conducted through a mechanism different than the dissolution-precipitation one, such as ion-exchange. Smičiklas et al. (2000), expended further on this notion. They explained that through an increase of the pH to the point where its value becomes higher than pH_{PZC} (point of zero charge) of Hap, the latter's surface turns negative leading to a growth in electrostatic attraction forces acting between the surface and the cations present in metalized water, thus resulting in enhanced metals immobilization at higher pH.

3.1.2. Nuclear waste management

One of the emerging technologies for the remediation of radionuclides contaminated sites, as well as the safe management of long-lived nuclear wastes by storage in deep geological repositories is the use of permeable reactive barriers (PRBs). This notion of PRBs consists in placing an adequate reactive solid in contact with the nuclear waste. This chosen material should be capable of immobilizing the contaminant either by a sorption process or by chemically reacting with the contaminant, forming thus a less harmful substance. However, the materials selected to be utilized as PRBs need to conform to certain standards that are required of them, in order to be considered viable options for radioactive waste clean-up. These critical properties are the following: high retention capacity and chemical durability, or in other terms, an irreversibility of the retention process.

Since hydroxyapatite is able to immobilize various heavy metals into its structure via its ion-exchange properties or through a dissolution-precipitation mechanism, and since these apatitic sequestered metals are generally recognized as stable and resistant to leaching, Hap appears as an attractive PRB material. Besides, seeing as hydroxyapatite has a low cost and is widely available in the environment, its use as radionuclide sorbent seems like a cost-effective choice of PRB. Among the most problematic and common radionuclides, we can distinguish U, Cs, Sr and I, all of which were able to be efficiently removed by Hap (Hasan et al., 2003; Fuller et al., 2002; Sasaki and Goto, 2014; Coulon et al., 2017), along with other radionuclides such as Np, Am, Pu and Co (Rigali et al., 2016). In fact, hydroxyapatite was found to exhibit a higher activity towards uranium removal compared to granulated activated carbon based sorbents confirming its great potential in the treatment of uranium contaminated sites (Coleman et al., 2003). While some further investigations remain to be seen to, regarding the sorption mechanisms that are involved in the radionuclides' confinement in the apatitic matrix, as well as the Hap's leaching properties in relation to different radionuclides, there is no doubt that hydroxyapatite constitutes a viable candidate as repository nuclear waste form.

3.2. Inorganic elements removal

Just as heavy metals pose a major threat to human health, and to both animals and plants' well-being, some inorganic elements can be as equally dangerous. Such elements, qualified by the term of "trace elements", while considered to be beneficial, and even essential to living organisms in small concentrations, become severely poisonous when they exceed the recommended permissible level. A typical trace element is fluoride, whose positive impact on teeth is widely known. However, above a limited concentration, fluoride causes grave complications resulting in dental and skeletal disorders, as well as the development of lesions in different body organs. Many fluoride sorbents have been investigated and examined over the years, such as activated carbon, natural zeolites, activated alumina and others, yet were still found lacking due to their high upkeep costs, their unsatisfactory fluoride sorption performance (efficiency and selectivity), and finally adverse impact on water quality, all of which would raise the cost of treatment even more (Gao et al., 2009a). Hence, hydroxyapatite stands out as an attractive option since it is a natural mineral component and so it can be easily produced from animal waste materials, which makes it economically practical and vastly available. Besides, Hap is known to possess high adsorption capacities and has no unfavorable effect on water quality. That is why hydroxyapatite has been used as a fluoride

sorbent in contaminated waters.

It proved to be very efficient according to several studies on fluoride adsorption by Hap material in aqueous solutions (Gao et al., 2009a; Poinern et al., 2011; Mourabet et al., 2015; Gao et al., 2009b; Fan et al., 2003). Indeed, in a study conducted by Fan et al. (2003) where several materials were tested at a natural pH (pH = 6) in order to assess their fluoride removal capacity, hydroxyapatite was shown to have the highest uptake of fluoride among all the examined adsorbents. The adsorption capacities of the tested materials followed the order: Hydroxyapatite > Fluorspar > Quartz activated using ferric ions > Calcite > Quartz. It should be emphasized as well, that while hydroxyapatite was able to adsorb over 90% of fluoride present in the solution, the second best adsorbent could only remove about 25% of F^- from the tested solution, evidencing thus Hap's excellent and superior sorption properties. In addition, Poinern et al. (2011), found that subsequent to the removal of fluoride, the obtained pH of the solution at equilibrium was of 6.6 which is within the standard pH range for potable water. This is extremely useful seeing as there would be no further need to adjust the pH for possible human consumption. Also, the study of Gao et al. (Gao et al., 2009a), showed that the de-fluoridation efficiency was size-dependent, meaning that Hap with smaller particle size were able to better remove fluoride than their bigger particle sized counterparts; this is noticeably outlined in Fig. 6. Most importantly, in the work conducted as well by Gao et al. (2009b), biogenic apatite and treated biogenic apatite exhibited comparable sorption performances to synthetic Hap, supporting the prospect of using hydroxyapatite prepared from waste materials in this process of fluoride decontamination.

Another trace element, whose consumption is both essential and dangerous, depending on its concentration, is selenium. This element, or more precisely its more mobile anion, selenite (SeO_3^{2-}), has been proven to be efficiently adsorbed on hydroxyapatite surface (Kongsri et al., 2013; Monteil-Rivera et al., 2000). In the case of selenite, the reason behind Hap excellent ability to immobilize selenium in contaminated soils is, other than its high stability and low water solubility, its capacity to exchange its own anions (phosphate groups) with the contaminant (selenite anions). In fact, Monteil-Rivera et al. (2000) were able to confirm through experimental techniques that the selenium derived from the selenite captured by Hap, was localized in the normally phosphorus occupied sites. In addition, these authors also observed that the removal of selenite was lessened in the presence of phosphate in the solution. However, this contaminant's sorption was improved by the presence of additional Ca ions in the solution, an occurrence which is highly likely in the case of natural waters, making this behavior of Hap advantageous. On a final note, Kongsri et al. (Kongsri et al., 2013) who prepared Hap from fish scales, making this material even more cost-effective, found it to be an efficient adsorbent of selenite, and thus a viable candidate for wastewater treatment, which goes to show that not only is synthetic Hap an extremely promising material for inorganic elements removal, but its extraction from natural sources offers a similarly efficient yet less expensive alternative choice.

3.3. Organic compounds adsorbent

Among the most commonly encoutered toxic organic compounds, we cite dyes, contaminants which are heavily discharged by textile industries, and that are often released into the water systems, generating great environmental concern due to their toxicity, mutagenicity, non-biodegradability and the visibility problems they create. Amidst available adsorbents, the use of hydroxyapatite for the management of wastewater dye pollution represents a clean, non-toxic and an environmentally friendly choice, especially when prepared from animal waste products. That is what occurred in the work conducted by Adeogun et al. (2018), in which these authors utilized a poultry eggshell derived Hap to eliminate Reactive Yellow 4 (RY4) dye, and found it to be an excellent inexpensive adsorbent of RY4 contaminants. Hap's ability to satisfactorily remove textile dyes was again showcased in a different study (Barka et al., 2011) that demonstrated hydroxyapatite's potential in physisorbing another reactive dye, Reactive Yellow 84, from the media.

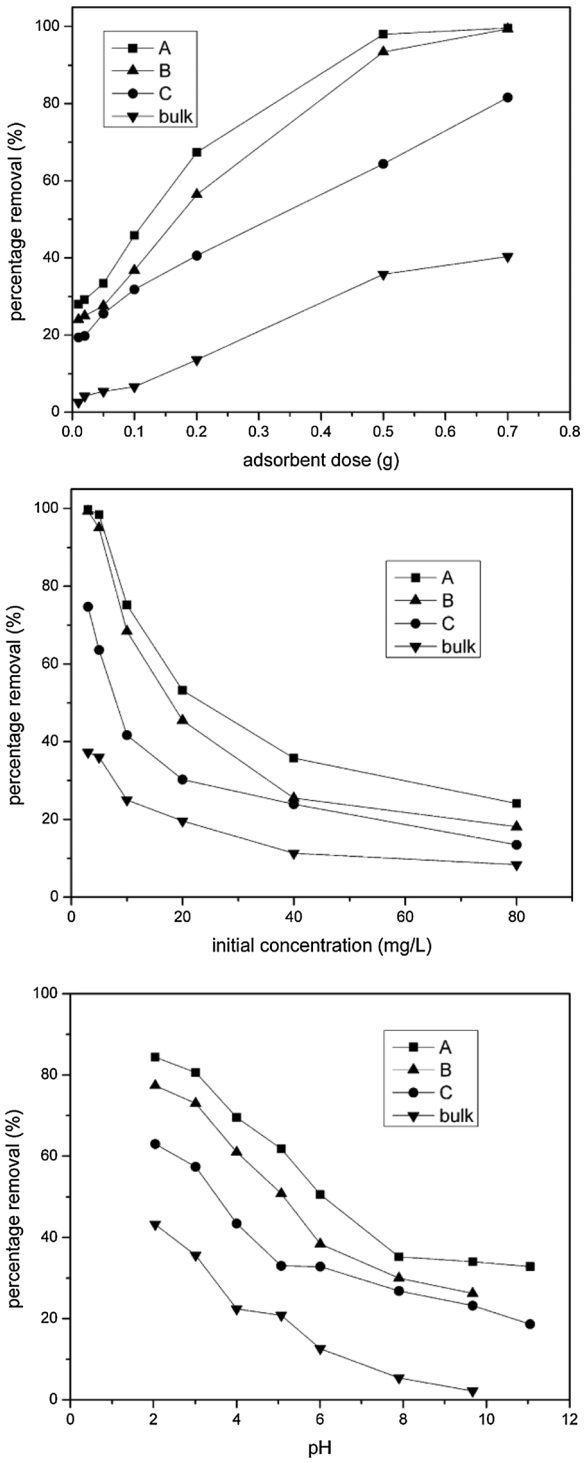


Fig. 6. (Top) Effect of adsorbent dose, (Middle) effect of initial fluoride concentration, and (Bottom) effect of pH on fluoride removal by Hap with different particle sizes (A: 48.2 nm, B: 62.8 nm, C: 97.9 nm and bulk: largest particle size). From reference (Gao et al., 2009a).

Other than organic dyes, the adsorption of fulvic acid (FA) was examined as well, when using a hydroxyapatite material as adsorbent (Wei et al., 2015). FA's abundant presence in consumable water is extremely harmful, since, in addition to causing disorders all on its own, it also lessens the efficiency of water purification. Moreover it can react

Table 1
Comparison of FA adsorption capacities of various sorbents. Adapted from reference (Wei et al., 2015).

Adsorbent	Q_0 (mg/g)
Poorly crystalline Hap	90.20
Modified zeolite	9.8
Modified vermiculite	12-18
Bacillus subtilis	0.71
Activated sludge	0.24
Chitosan hydrogel beads	2.933
Carbon nanotubes	24.57
SiO_2 particles	28.63-490.5
Mg/Al layered double hydroxides	54.3-294.1

with the compounds used to treat consumable water, leading to cancerogenic by-products. Hap was found to be a viable and recyclable adsorbent for FA elimination from aqueous media. Furthermore, the mechanism of FA adsorption over Hap was ascribed to the surface complexation between the oxygen atom of functional groups of FA and calcium ions of hydroxyapatite. Also, Hap's adsorption efficiency increased with the decrease of its crystallinity. Most importantly, when its adsorption capacity was compared to those of formerly reported adsorbents, it was apparent that Hap exhibited a higher efficiency than many. Table 1 outlines the FA adsorption capacity values of the stated materials, obtained from various works.

Finally, Hap was shown to possess a great potential for the elimination of additional organic pollutants, namely nitrobenzene, a toxic and carcinogenic organic chemical, often discharged in the effluents originating from explosives, pesticides and plastic productions, and whose elimination from contaminated media by the use of hydroxyapatite is possible over a vast range of concentrations (Wei et al., 2010). Also, studies showed that hydroxyapatite is capable of an efficient and rapid physisorption of phenol, an organic pollutant largely generated by coal conversion, petroleum refining and plastic industries, whose removal from wastewaters is an ecological necessity (Lin et al., 2009).

In addition to apatites' numerous applications as adsorbents for the treatment of contaminated soils and waters, one more vital environmental aspect of hydroxyapatite is its considerable contribution in the field of catalysis.

4. Hap in catalytic reactions

4.1. As a catalyst

4.1.1. Biodiesel production

Always in the aim of supporting a sustainable development, the substitution of fossil fuels, the reservoirs of which are rapidly decreasing, with biodiesel, an alternative fuel source, is a promising solution for sustainable energy production. Conventionally, homogeneous base/acid catalysts are used in the biodiesel synthesis process. However, due to the problems these type of catalysts generated (difficulty of separation, non-recyclability, …), researchers turned to heterogenous catalysts in order to simplify and lower the cost of production (Farooq et al., 2015).

Among these heterogeneous catalysts, hydroxyapatite shows a good activity towards biodiesel production because of its acid-base properties, and more specifically in this case, its catalytically active basic sites (Buasri et al., 2015), such as calcium oxide sites (Obadiah et al., 2012; Smith et al., 2013). What is more, a quality analysis of biodiesel produced when using Hap as catalyst was performed by Gupta et al. (Gupta and Agarwal, 2017), and when the results were compared with ASTM D67 Standard, they were found within the prescribed limit, as reported in Table 2.

Moreover, with the objective of reducing the cost even further, studies were conducted on the use of Hap derived from waste for the production of biodiesel. These studies have shown hydroxyapatite catalysts developed from waste materials to exhibit high catalytic activity with good biodiesel yield and good recyclability (Farooq et al., 2015; Buasri et al., 2015; Obadiah et al., 2012; Smith et al., 2013; Gupta et al., 2018; Yan et al., 2016). It is also worth mentioning that in a study conducted by Yan et al. (2016) on the utilization of hydroxyapatite-supported CaO-CeO_2 catalyst for biodiesel production, the biodiesel yield over pig bones derived hydroxyapatite catalyst (83.5%) was found to be comparable to that obtained over a series of CaO-CeO_2 catalysts supported on this animal waste derived Hap (85.4% < yield < 91.8%) and depending on the calcination temperature of the CaO-CeO_2 impregnated catalyst, sometimes even slightly higher (yield = 82.8% when calcined at 800 °C). All of the above goes to show the economic and ecological gain to be had by using hydroxyapatite as a catalyst in biodiesel production.

Table 2
Quality analysis of biodiesel. Adapted from reference (Gupta and Agarwal, 2017).

Properties	Unit	Biodiesel from HAP	ASTM Standard
Density	(mg/mL)	0.88	0.86-0.90
Kinematic viscosity	at 40 °C (cSt)	5.72	1.9-6.0
Acid value	(mg of KOH/mg of oil)	0.4	0.5
Cloud point	°C	9	−3 to 12
Pour point	°C	3	−15 to 10
Flash point	°C	155	130-170

4.1.2. VOC oxidation

Volatile organic compounds (VOCs), emitted from a variety of sources including industrial processes and transportation activities, constitute a well-known class of air pollutants. One of the most effective, inexpensive and environmentally compatible solutions for the removal of these pollutants is their total oxidation in the presence of a catalyst. The advantages of catalytic oxidation on thermal oxidation are the reduction of energy consumption since the catalyst lowers the oxidation temperature, and the promotion of efficiency since it directs the selectivity towards the desired products (CO_2 and H_2O).

Among said VOCs, we recognize formaldehyde (HCHO), a short-chain oxygenated compound which is classified as being a carcinogenic VOC and thus a major hazard to human health. Although HCHO catalytic oxidation is usually carried out over precious metal catalysts such as platinum or palladium, recent studies have shown that hydroxyapatite is not just catalytically active in the oxidation of formaldehyde but that it also exhibits an excellent performance at room temperature, which makes this non-precious metal catalyst an ideal candidate for HCHO removal (Xu et al., 2010; Sun et al., 2014). Furthermore, when the activity of hydroxyapatite was compared with that of a supported precious metal catalyst, Pd (3 wt%) / γ-Al_2O_3, results revealed that at room temperature the conversion of formaldehyde was ca. 45% for Hap, only slightly lower than for the Pd catalyst (ca. 57%). However, while formaldehyde conversion over Hap remained stable at 45% for the first 2 h of reaction at room temperature before dropping to 28% after running for 10 h, the catalytic activity of Pd-based catalyst decreased rapidly from 57% to 33%. Finally but most importantly, Hap displayed higher mass-specific and turnover rate values than Pd (3 wt %) / γ-Al_2O_3; all of which goes to demonstrate hydroxyapatite's good catalytic performances (good activity and stability) when it comes to HCHO oxidation under ambient conditions (Xu et al., 2010). It should be noted that Hap's catalytic activity was attributed to the hydroxyl groups bonded with the channel Ca^{2+}. Indeed, these groups would play an important role in activating/oxidizing the formaldehyde compound, assisting thus the catalytic process.

Hap was, in addition, tested as a possible catalyst for the oxidation of other VOCs, namely gaseous toluene, ethyl acetate and iso-propanol (Nishikawa et al., 2012), and was found equally active in the oxidative decomposition of these volatile organic compounds at 400–500 °C. In fact, in this case, the oxidation of the studied organic compounds was instigated by the activation of oxygen due to the electron trapped on vacancy in Hap, this electron being generated by thermal excitation.

On another note, chlorinated organic compounds, whose treatment is vital in order to prevent their harmful effects on the environment and health, have also found a viable catalyst option in hydroxyapatite. In fact, calcium deficient Hap manifested a good performance in the oxidative decomposition of trichloroethylene vapor at 400–500 °C and was able to capture as well the Cl species since only a small amount of HCl was found in the effluent gas (Nishikawa et al., 1993; Nishikawa and Monma, 1993). It was supposed that Cl^- would replace OH^- in hydroxyapatite, producing thus chloroapatite. The same was shown to be true in the study conducted by Nishikawa et al. (Nishikawa and Monma, 1994), where chlorobenzene was oxidatively decomposed at 400–500 °C, over calcium deficient Hap (DAp), with the major part of Cl being seized by the calcium phosphate catalyst according to the data reported in Table 3.

Just as Hap was proven to be a performant catalyst in the previously mentioned fields, it was also revealed to display good photocatalytic activity whether combined with other photocatalytic materials, or undoped. We will presently examine the use of hydroxyapatite as photocatalyst in environmental remediation procedures.

4.2. As a photocatalyst

4.2.1. Undoped, single phase Hap

Hydroxyapatite was able to achieve photocatalytic decomposition under UV irradiation of dyes (whose harmful effects were previously cited), such as methyl orange (Liu et al., 2016), methylene blue (Shariffuddin et al., 2013), and calmagite (Reddy et al., 2007). What is more, Hap was also an efficient photocatalyst for degradation of the 17α-methyltestosterone (MT) hormone under solar and ultraviolet radiation (Savaris et al., 2018), a hormone used in fish farming, but whose heavy use, and subsequent water contamination with it, can eventually lead to the deregulation of all hormonal systems in humans and animals as well. Savaris et al. (Savaris et al., 2018) showed that the reduction in 17 α-methyltestosterone absorbance was faster on Hap undoped than when doped with nickel and copper, as well as faster than on a TiO_2 catalyst. The results are presented in Table 4.

In addition, Hap can be applied for the photocatalytic decomposition under UV irradiation of dimethyl sulfide (Tanaka et al., 2012; Nishikawa, 2004a), a toxic organic compound that causes skin, eye and respiratory irritation, and has a very unpleasant odor. Let us note that studies indicated that the photocatalytic activity of Hap is most likely correlated with the crystallinity toward the a-axis of Hap crystal, since hydroxyapatite crystals which had a lower crystallinity toward the apatite a-axis, but a similar crystallinity toward the c-axis, exhibited a

Table 3
Cl^- amounts in fresh and reacted Dap.[a] Adapted from reference (Nishikawa and Monma, 1994).

	Cl^-/DAp (mg. g^{-1})		A/B[c]
	(A) Found	(B) Calcd[b]	%
Fresh	None	–	–
Reacted	1.6	1.86	86

[a] Reaction conditions: chlorobenzene = 40.1 ppm (v/v); DAp = 1 g; reaction temperature = 450 °C.
[b] Theoretical amounts when the DAp was completely chlorinated with chlorobenzene reacted.
[c] Cl^- amount in DAp to Cl amount in decomposed chlorobenzene.

Table 4
Reduction in 17 α-methyltestosterone absorbance with different catalysts, in one hour of irradiation. Adapted from reference (Savaris et al., 2018).

Catalyst	Method	Reduction (± 1 %)
Hap without doping	CP[1]	100
Hap without doping	HP[2]	43
Hap doped with Ni	HP[2]	43
Hap doped with Cu	HP[2]	39
TiO_2	–	33
UV[3]	–	28

[1] conventional precipitation.
[2] homogeneous precipitation.
[3] without catalyst.

decrease in the photocatalytic activity compared to those with a higher crystallinity toward the a-axis (Nishikawa, 2004a). Most importantly, concerning the mechanism that enables Hap to act as a photocatalyst under UV irradiation, it was simply explained by the following process: the electronic state of the surface phosphate group will be altered and produce a vacancy on hydroxyapatite, and then an electron transfer occurs from the vacancy formed in apatitic structure to atmospheric oxygen present on Hap resulting in the formation of $O_2^{\cdot -}$ radicals, which will oxidize the organic compounds (Nishikawa, 2003, 2004b). Regarding the energy wavelength range in which Hap can absorb, a previous study conducted by De Araujo et al. (2010) has shown that pure hydroxyapatite presents optical absorption in the UV region 200–340 nm with a strong band below 247 nm. However, it should also be mentioned that when doped with other elements, Hap's absorption spectrum undergoes significant changes. For example, the incorporation of metals such as Cr^{3+} or Fe^{3+} in the apatite lattice produces absorption bands in the spectral interval going from UV to visible (200–800 nm), whereas doping Hap with Zn^{2+} leads to absorption features in the UV–vis region 213–420 nm, which is similar to that obtained for pure TiO_2 (268–419 nm).

These modifications in the absorption properties of doped hydroxyapatites can prove to be very beneficial for the photocatalytic activity, depending on the envisioned application. Therefore, in the upcoming section we will move on to the use of Hap, still in photocatalysis, but in combination with other photocatalytic materials, employed in various photocatalytic applications.

4.2.2. Combined with other photocatalytic materials (doped Hap and Hap-containing composites)

4.2.2.1. Photocatalytic degradation of organic compounds. As seen for several times so far, ones of the most common organic pollutants that contaminate wastewaters nowadays are synthetic dyes. Their removal is required in order to avoid the many adverse effects they can have on aquatic and human life. While titanium oxide is a widely used photocatalyst because of its chemical stability and excellent activity, one of its recognized downsides is its weak adsorption capacity when it comes to some organic contaminants. Therefore, a simple and cost-effective solution would be to combine this highly active material to another that would be endowed with good adsorption properties. Seeing as hydroxyapatite is well known for its high adsorption ability, and since it has been revealed to exhibit good photocatalytic performances in the degradation of organic pollutants (refer to section 4.2.1.1), an association of TiO_2 and Hap looks promising. Indeed, the combination of TiO_2/Hap proved to be effective in the photodegradation of methylene blue (Piccirillo et al., 2017; Ji et al., 2009; Anmin et al., 2006; Sahibed-dine et al., 2017), and the degradation of rhodamine B (Han et al., 2016). Moreover, several studies confirmed that the biphasic material TiO_2/Hap, displays a superior photocatalytic performance than the corresponding single-phase catalysts (TiO_2 and Hap) (Piccirillo et al., 2017; Ji et al., 2009; Anmin et al., 2006; Sahibed-dine et al., 2017). In fact, Piccirillo et al.

(Piccirillo et al., 2017) reported a 50% increase in the methylene blue photodegradation activity, when TiO_2 was combined with hydroxyapatite. Other Hap based composites have also been prepared in the aim of decreasing the pollution caused by organic dyes. An example is the coupling of the Ag_3PO_4 and Hap, tested in photodegradation of rhodamine B (Chai et al., 2015). The synthesized Ag_3PO_4/Hap composite improved by ten times the activity of pure Ag_3PO_4. Another example of a modified Hap catalyst employed for the removal of dyes, is an amorphous Fe(III)-substituted hydroxyapatite compound, whose photocatalytic activity in the degradation of rhodamine B was good and similar to that of crystal semiconductors Bi_2WO_6 and $BiVO_4$ (Liu et al., 2014).

Equally as toxic, and even more dangerous than organic dyes, are pharmaceutical products which are, frequently, inadequately discarded, resulting in their accumulation in the environment, hence endangering both animals and humans' well-being. One of the most encountered compounds amid these products is diclofenac (DCF), which was shown to be effectively photodegraded by the multiphasic hydroxyapatite–TiO_2 material, a photocatalyst that succeeded in diminishing the toxicity of the contaminated water considerably (Murgolo et al., 2018; Brazón et al., 2016). The Hap-titania photocatalyst manifested too an excellent degradation efficiency of the micropollutant fluoxetine, the maximum degradation performance reaching 100%, with contaminant and photocatalyst concentrations corresponding to 2 ppm and 4 g/L, respectively (Brazón et al., 2016). Furthermore, when El Bekkali et al. (2018) assessed zinc oxide-hydroxyapatite nanocomposites for the photodegradation of two antibiotics, ofloxacin and ciprofloxacin, in solution, these Hap-containing composites proved to be highly efficient and even displayed a greater activity compared to the oxide phase alone as can be seen in Fig. 7.

Other organic pollutants such as pentachlorophenol (Xie et al., 2013) and formaldehyde (Hu et al., 2018) were efficiently photodegraded as well over TiO_2/Hap composite and Cr(III)-doped Ti-Hap particles were capable of carrying out the photocatalytic decomposition of acetaldehyde (Wakamura et al., 2011).

In addition to the photocatalytic degradation of organic compounds, modified Hap materials proved to be active in photocatalytic NO_x removal.

4.2.2.2. Photocatalytic NO_x removal. Nitric oxides (NO_x) produced during fuel combustion processes are a major safety concern, especially nitric monoxide NO and nitrogen dioxide NO_2 which are known to be most harmful to the human health and the environment. They are at the origin of numerous environmental problems, such as acid rain, the formation of smog, the formation of tropospheric ozone, and the destruction of animal and plant species. While TiO_2 is a performant photocatalyst, it presents considerable inconveniences which are its low adsorption ability for contaminants (as mentioned previously), and its high recombination of photo-induced electron-hole pairs, all of which is detrimental for a good photocatalytic activity. This is exactly where hydroxyapatite comes to the rescue. Indeed, it was demonstrated on several occasions (Giannakopoulou et al., 2012; Yao et al., 2017; Mitsionis et al., 2011) that a TiO_2/Hap composite showed a superior photocatalytic activity compared to pure components (TiO_2 and Hap), and that a higher NO removal was achieved thanks to this promising combination. Not only that, but also, the production of the toxic intermediate NO_2 was considerably lessened over the prepared titania-hydroxyapatite composite.

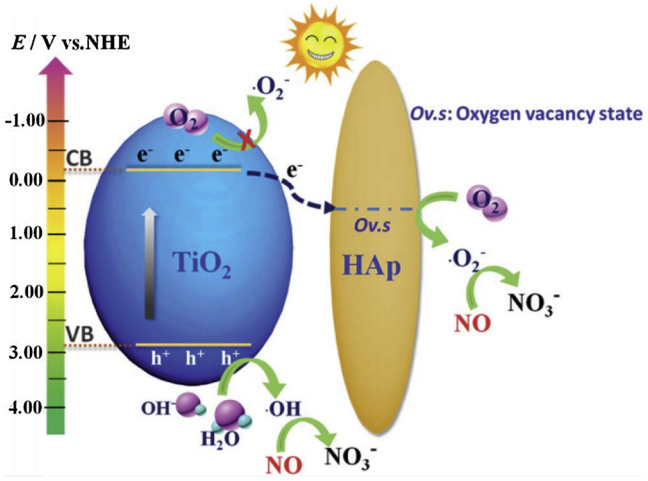


Fig. 8. Photocatalytic mechanism scheme of TiO_2/Hap under simulated solar light irradiation. From reference (Yao et al., 2017) - Published by The Royal Society of Chemistry.

This welcomed and improved behavior was credited to an enhanced chemisorption of NO due to a greater amount of surface OH groups, as well as to higher separation efficiency and faster transfer of the photogenerated electron-holes pairs as shown in Fig. 8. Furthermore, recyclability tests showed the TiO_2/Hap material to possess good photocatalytic stability.

4.2.2.3. Photocatalytic bactericidal activity. Bacterial pathogens found in consumable waters represent a recurrent environmental and health issue. Resorting to photocatalysis constitute a suitable solution for the disinfection of bacteria-contaminated waters. Generally, TiO_2 has been commonly used as photocatalyst in bactericidal applications. Nonetheless, in this field as well, combining Hap with TiO_2 tremendously enhanced the bactericidal activity (Pratap Reddy et al., 2007; Hu et al., 2007). Such an occurrence was attributed to two factors: Hap's excellent ability in adsorbing bacteria (contrary to titania

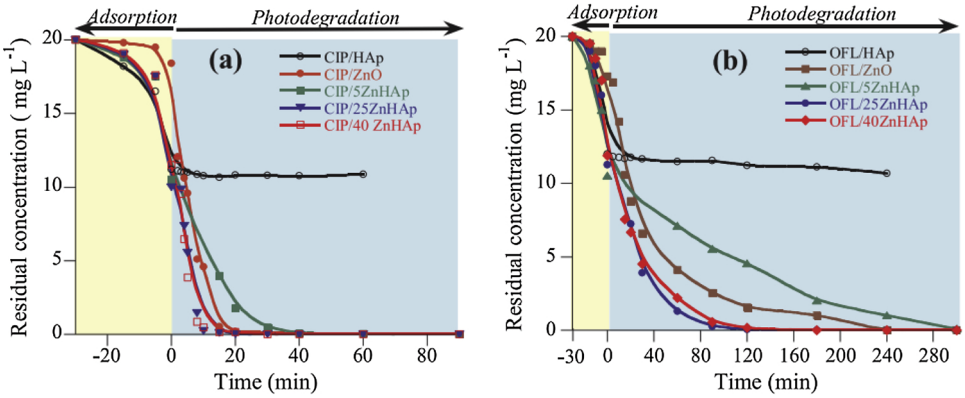


Fig. 7. Kinetics of (a) ciprofloxacin and (b) ofloxacin removal (q_e) by the *w*ZnHAp composite powders heated at 500 °C compared to pure HAp and ZnO during a first 30 min period in the dark followed by irradiation using a 125 W UV A-B-C lamp. From reference (El Bekkali et al., 2018).

for which no bacterial adsorption is observed), associated with its photocatalytic property. The association of these two properties imparts Hap with the qualification of a "sense and shoot" catalytic system, meaning that it is able to simultaneously sense and destroy these pathogenic compounds (Pratap Reddy et al., 2007), a dual role that makes Hap a very desirable material for the detoxification of bacteria-containing waters.

However, what is even more interesting was that a co-precipitated Hap doped with Ti material, was shown to produce $O_2^{\cdot -}$ not only under weak UV irradiation, but also at ambient temperatures in the dark, whereas pure Hap and TiO_2 catalysts did not exhibit any catalytic activities at ambient temperatures in the dark (Hu et al., 2007). While it has been established that $O_2^{\cdot -}$ radicals could be generated on Hap by heat treatment or UV irradiation, this does not explain HapTi's capacity to manifest a photocatalytic activity in the dark and at room temperature. This phenomenon was rationalized by a substitution of calcium (II) in the crystal of Hap by Ti(IV), which is likely what caused the occurrence of an oxygen vacancy in hydroxyapatite, seeing as the valency of Ti(IV) is higher than that of Ca(II).

Up until this moment, we have reported the use of Hap in catalysis as a catalyst and photocatalyst, and demonstrated its added value in each of these departments. However, one important aspect of the catalytic applications of Hap remains to be seen, which is none other than the use of hydroxyapatite as a support for an active phase in various environmentally oriented catalytic reactions.

4.3. As a support for an active phase

4.3.1. Oxidation of toxic pollutants

Due to its textural and structural characteristics, hydroxyapatite is of considerable interest as catalyst's support in numerous oxidation processes. In fact, in alkane oxidation reactions such as methane oxidation, Hap's tunable acidic and basic properties were found to be of particular consequence on the catalytic activity. Previous studies had shown, that catalysts' basic sites could be held responsible for the activation of methane. This, therefore, explains the choice of hydroxyapatite as metal carrier in several works (Sugiyama et al., 1998, 1996; Sugiyama et al., 1997; Boukha et al., 2007a). A study conducted by Boukha et al. (2007a), using Pd loaded Hap, led to results with similar performance in methane's oxidation to that of conventional Pd/Al_2O_3 catalysts, thus, proving the apatite material's efficiency as a carrier in this reaction. In addition to hydroxyapatite's modulable acid/base properties, its relatively high surface area came into play in the oxidation of 1,2-dichloroethane, catalyzed by cobalt supported on Hap (Boukha et al., 2016). Tests showed that the good dispersion of cobalt active species, led to a significant improvement in the catalytic activity, when compared to bulk Co_3O_4 catalyst.

As for aromatics and aldehydes' oxidation, in a work conducted by Wang et al. (2015), hydroxyapatite was reported to enhance the thermal stability of gold against sintering. A detailed examination showed that apatite's phosphate groups were the source of gold nanoparticles stabilization at lower temperature ($\leq$400 °C), while hydroxyl group were at the origin of higher temperature stability ($\leq$600 °C). To better point out Hap's stabilizing effect, a comparison was made between Au/CeO_2/Hap and Au/CeO_2 catalysts, both calcined at 600 °C, in formaldehyde oxidation reaction. Results indicated a high HCHO conversion for the Au/CeO_2/Hap material (98% conversion) in opposition to Au/CeO_2 that only gave 5% HCHO conversion because of its poor stability in regard to sintering. Furthermore, toluene's total oxidation, assessed over various metals supported on hydroxyapatite, led to the conclusion of oxidation activity being related to the high dispersion of active species as well as the carrier's acid characteristics. In fact, the support's acidic centers heighten the prospect of an electrophilic attack of adsorbed oxygen, hence, the oxidation of toluene molecules; the electrons trapped in Hap's vacancies are considered as accountable for oxygen activation. Indeed, palladium loaded on hydroxyapatite were more performant than Pd supported on classical alumina in total toluene oxidation. The specific rates on apatites supports were four to six times higher even though the palladium content was lower on Hap (0.25 wt% of Pd on Hap vs 0.4 wt% of Pd on Al_2O_3) (Chlala et al., 2016a). This was also true when the active phase used was manganese. The toluene conversion increased when passing from Mn supported on alumina (Mn-Al) to the one supported on hydroxyapatite (MnNit-Hap and MnAc-Hap), and that no matter the nature of the precursor used (manganese nitrate: MnNit or manganese acetate: MnAc) to incorporate manganese active species on Hap (Fig. 9) (Chlala et al., 2016b). Hydroxyapatite's acidic properties were also found to be responsible for methanol's activation in a study conducted by Aellach et al. (2010) over calcium-deficient and stoichiometric hydroxyapatites promoted by cobalt, for the catalytic oxidation of methanol. Indeed, the authors found that while the redox properties of Co_3O_4 entities formed on the catalyst's surface were mainly responsible for the catalytic activity of the supported material, an enhancement in the catalytic performances could be noted when replacing a stoichiometric Hap support with a calcium-deficient one. The specific role of this Ca-deficient support in that particular case was explained by the presence of surface acid sites in the form of HPO_4^{2-} species and surface cationic vacancies, believed as accountable for methanol activation at low temperature, resulting thus in improved catalytic activity. Moreover, Hap's ion-exchange capacity, as well as its great recyclability permitted for a synthesized Cu doped Hap catalyst to be reused in the oxidation of formaldehyde without significant loss in its catalytic activity (Qu et al., 2014).

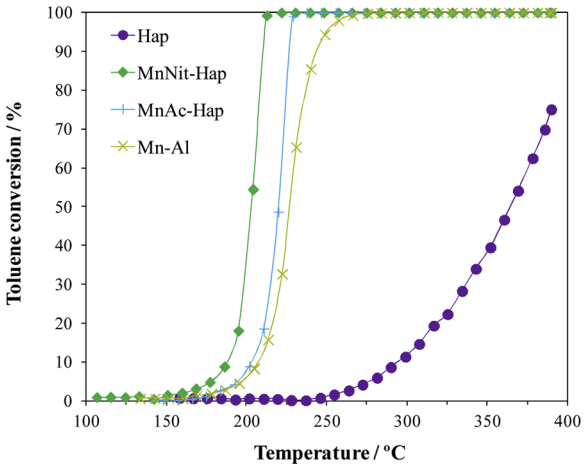


Fig. 9. Toluene conversion over the catalysts (GHSV = 30,000 mL.h^{-1}. g^{-1}; 800 ppmv toluene in air). From Reference (Chlala et al., 2016b).

Finally, studies for the applicability of hydroxyapatite supported gold in CO elimination processes, were conducted by several researchers (Boukha et al., 2017; Huang et al., 2011; Domínguez et al., 2009; Phonthammachai et al., 2008; Wang et al., 2014; Venugopal and Scurrell, 2003; Zhao et al., 2011, 2013). The aim was to find a support whose properties would amplify the reactivity of nanosized gold. As already mentioned above, Hap succeeded in enhancing the stability of Au nanoparticles creating a highly durable catalyst. This renders the apatitic material an ideal alternative to metal oxide supports such as $CuMn_2O_3$ and TiO_2, hindered by a rapid deactivation caused by Au crystals' growth; these carriers becoming thus, unsuitable for long term use (Phonthammachai et al., 2008). What is more, Domínguez et al. (2009) revealed Hap's implication in the enhancement of the catalytic activity, in the oxidation of CO at room temperature. Apparently, structural vacancies in the apatite structure can activate oxygen to produce peroxide species which are behind CO's room temperature oxidation.

4.3.2. Reduction of NO_x

An often studied reaction that uses as host the apatitic support, is nitrogen oxides' reduction (Tounsi et al., 2011; Jemal et al., 2012; Kumar et al., 2008; Huang et al., 2015, 2016; Lin et al., 2015; Schiavoni et al., 2018; Campisi et al., 2019). On the one hand, the contribution of hydroxyapatite to the catalytic process comes in the form of a novel material capable of securing a good dispersion of the active phase. While Tounsi et al. (Tounsi et al., 2011; Jemal et al., 2012) established in their work, that the highly dispersed CuO particles on Hap surfaces were responsible for the NO conversion in the low temperature range, Kumar et al. (2008), demonstrated that well dispersed Ag_2O on the apatite carrier led to the best DeNOx activity compared to a series of traditionally supported catalysts (Al_2O_3, TiO_2, SiO_2, ZrO_2, TiO_2–ZrO_2 and Ga_2O_3). However, it is worth mentioning that depending on the metal precursor used to introduce the metallic phase, the activity and selectivity in the NH_3-SCR process can significantly vary due to a modification in hydroxyapatite's structural features and surface composition. Indeed, in a study conducted by Schiavoni et al. (2018) over Cu-functionalized hydroxyapatites in NH_3-SCR reaction, these authors found that when copper acetate was employed as Cu-phase precursor (instead of copper nitrate or copper chloride) it caused some alteration of the Hap surface resulting in enrichment with carbonate groups, which proved to be unfavorable for the SCR activity.

On the other hand, an equally important feature of Hap is its basic properties. In fact, rhodium loaded on hydroxyapatite exhibited superior catalytic activity in N_2O's decomposition than Rh/Al_2O_3, Rh/TiO_2, and Rh/SiO_2, as is clearly apparent in Fig. 10. This was ascribed to a surface richer in basic sites in the case of Hap. It was postulated that the higher basicity of this carrier could improve rhodium's dispersion, which in turn, would lead to the enhancement of the catalytic activity (Huang et al., 2015).

This was also true in another study conducted by Huang et al. (2016), at the end of which, these researchers concluded that surface hydroxyls and the basicity of hydroxyapatite are beneficial for the decomposition of nitrous oxide. Lin et al. (2015) confirmed this as well, when they studied the performance of RhO_x/M–P–O (M = Mg, Al, Ca, Fe, Co, Zn, La) catalysts in the decomposition of N_2O. RhO_x/Hap showed the highest activity among the tested materials (Fig. 11) due, evidently, to its more basic sites. NO_2's conversion values at 275 °C, for the different RhO_x supported solids, which are presented in Table 5, validate the greater catalytic conduct of RhO_x/Hap.

4.3.3. Production of hydrogen

Nowadays, the search for a safe and efficient hydrogen storage technology is of the utmost importance, because, unlike fossil fuels, hydrogen is a green and sustainable energy carrier. Hydrides are a readily available hydrogen source, and can easily generate H_2 through a hydrolysis reaction. Recently, hydroxyapatite has aroused considerable interest in view of its potential use as catalyst support for such processes (Jaworski et al., 2013; Özhava and Özkar, 2015; Akbayrak et al., 2013; Rakap and Özkar, 2011, 2012; Durak et al., 2014; Celik et al., 2012), owing to its high ion-exchange ability and large surface area. In fact, ruthenium supported on hydroxyapatite proved to have superior reusability properties than other supports when compared to literature results (Fig. 12). Hydroxyapatite's notable support effect was further evidenced by the better results obtained in the case of a palladium loaded Hap catalyst for the hydrolysis of ammonia-borane, compared to other carrier materials such as γ-Al_2O_3.

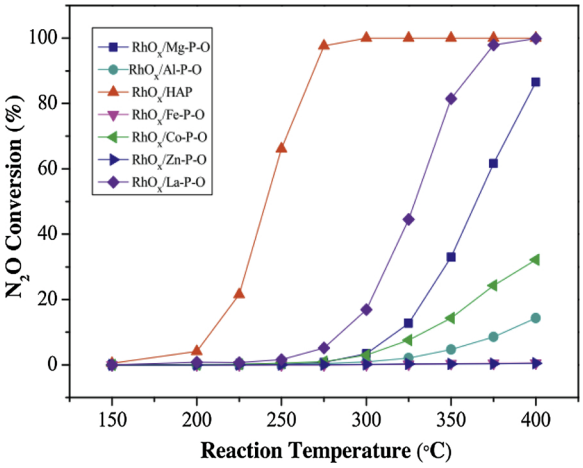


Fig. 11. N_2O conversion as a function of reaction temperature for RhO_x/M–P–O (M = Mg, Al, Ca, Fe, Co, Zn, La) catalysts. Reaction conditions: 0.5 vol.% N_2O in He; total flow rate = 60 cm^3/min; catalyst weight = 0.5 g. From Reference (Lin et al., 2015).

Table 5
Catalytic decomposition of N_2O over RhO_x supported on metal phosphates. Adapted from reference (Lin et al., 2015).

Catalyst	Rh content (%)	N_2O Conversion at 275 °C (%)
RhO_x/Hap	2.99	97.2
RhO_x/Mg-P-O	3.17	0.7
RhO_x/Al-P-O	1.50	0.4
RhO_x/Fe-P-O	3.17	0
RhO_x/Co-P-O	2.39	0.9
RhO_x/Zn-P-O	3.02	0
RhO_x/La-P-O	2.69	5.2

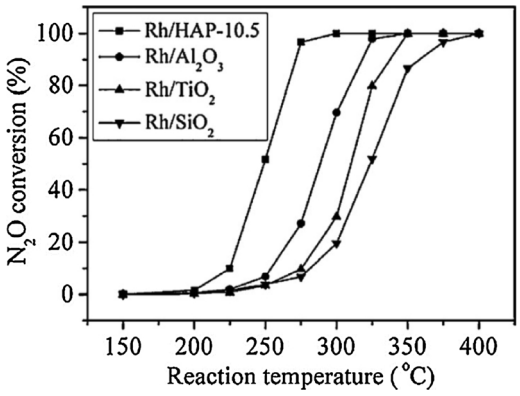


Fig. 10. Conversion of N_2O on Rh/HAP-10.5, Rh/Al_2O_3, Rh/TiO_2, and Rh/SiO_2 catalysts as a function of reaction temperature. From Reference (Huang et al., 2015).

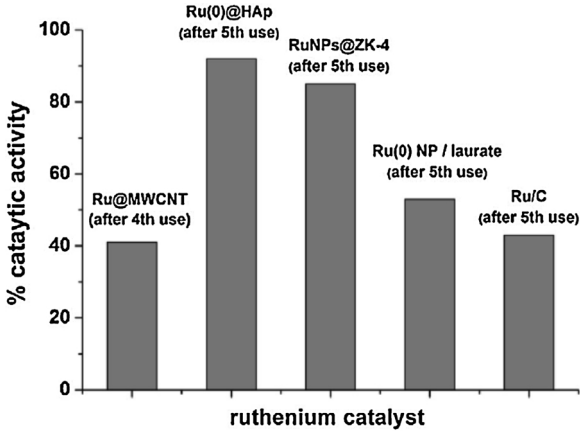


Fig. 12. The percentage of initial catalytic activity of various reported ruthenium catalysts after the reuse for the hydrolytic dehydrogenation of ammonia borane. From Reference (Akbayrak et al., 2013).

A different way of producing hydrogen is through methane conversion. Here as well, Hap proved to be a useful host material (Boukha et al., 2007b; Rêgo De Vasconcelos et al., 2016; Lee et al., 2002; Matsumura et al., 1994; Jun et al., 2004). The flexibility of the apatite structure provides it with the aptitude for tolerating various substitutions and ion exchanges in its framework, allowing the active species to occupy the position vacated, in most cases, by calcium ions. This resulted in excellent performance and enhanced stability (Rêgo De Vasconcelos et al., 2016). This support's remarkable properties were corroborated by the work of Jun et al. (2004). A salient difference was observed between the activity of nickel–calcium phosphate/hydroxyapatite catalyst and other Ni catalysts (NiO/SiO_2, NiO/Al_2O_3–TiO_2–CaO), suggesting an easier reducibility of Hap supported catalyst.

4.3.4. Desulfurization

The suitability of Hap as support for desulfurization of sulfur containing compounds was examined. Hydroxyapatites proved to be efficient carriers of NiMo sulfide catalysts, for desulfurization of thiophene (El Azarifi et al., 2005) and hydrodesulfurization of dibenzothiophene (Elazarifi et al., 2004). In those two processes, apatite supported NiMo showed higher activity than industrial alumina supported catalyst, despite having lower specific surface area. This was due to the presence of superficial HPO_4^{2-} groups and related surface defects, which would act as grafting sites of Ni-Mo oxides, thus, facilitating the dispersion of these active species. The contribution of the apatitic support to the catalyst's performance was evidenced by the improvement in sulfur removal, when going from a catalyst free system (22.7%), to a system comprised of only hydroxyapatite (45.8%) (Riad and Mikhail, 2012). This was believed to be the result of Hap's good adsorption properties that provide the required adsorption sites, in which, sulfur compounds' desulfurization could take place. Furthermore, when a composite consisting of TiO_2 whiskers and Hap nanotubes was inspected as support material for NiMo active phase, in the hydrodesulfurization (HDS) of dibenzothiophene, results indicated better catalytic activity in the case of NiMo/TiO_2-Hap, compared to NiMo/TiO_2 solids (Wang et al., 2016). This consolidated the role of Hap as a functional promoter for titania in the HDS reaction.

5. Concluding remarks and outlook

- Potentials of hydroxyapatite as a multifunctional material for environmental remediation

All of the aforementioned evaluation and appraisal of Hap's role in environmental remediation culminate in one single fact: hydroxyapatite is a perfectly suitable, and highly promising bio-inspired material for various environmental applications. The unique features of this material accord it with exceptional carrier traits resulting in the enhancement of performances in the aimed for fields (adsorption, catalysis). Therefore, this review which was devoted to the display of Hap's outstanding properties and their subsequent use in removal of pollution from contaminated waters, soils and air, helped establish the benefits gained from the use of such material, on its own or as a host to different active species.

- Utilization of a zero-waste concept

An interesting future matter to examine is finding possible ways of utilizing used Hap adsorbents, once their role, as metal removal materials for example, has been fully achieved. A most plausible area of application of these metal containing hydroxyapatite compounds would be in catalysis. In other words, Hap would be acting here as a support for an active phase. This would be a most original manner with which to convert used materials into value added products, and thus apply a zero-waste concept allowing to dispose of waste materials all while protecting the environment.

In our following work, we will focus our research on employing Hap as a support to an active phase in oxidation catalysis. An optimization of the preparation method and experimental conditions will be a vital component in our upcoming research since it will have a great impact on our synthesized catalysts' performances.

Declaration of Competing Interest

The authors declare no conflict of interest.

Acknowledgements

This research has been supported by an Interreg V France-Wallonie-Vlaanderen project entitled "DepollutAir". Maya Ibrahim thanks the Lebanese University for their support through a PhD grant.

References

Abdulrahman, I., Tijani, H.I., Mohammed, B., Saidu, H., Yusuf, H., Ndejiko Jibrin, M., Mohammed, S., 2014. From garbage to biomaterials: an overview on egg shell based hydroxyapatite. J. Mater. 2014 6 pages.
Adeogun, A.I., Ofudje, E.A., Idowu, M.A., Kareem, S.O., Vahidhabanu, S., Babu, B.R., 2018. Biowaste-derived hydroxyapatite for effective removal of reactive yellow 4 dye: equilibrium, kinetic, and thermodynamic studies. ACS Omega 3 (2), 1991–2000.
Admassu, W., Breese, T., 1999. Feasibility of using natural fishbone apatite as a substitute for hydroxyapatite in remediating aqueous heavy metals. J. Hazard. Mater. 69 (2), 187–196.
Aellach, B., Ezzamarty, A., Leglise, J., Lamonier, C., Lamonier, J.-F., 2010. Calcium-deficient and stoichiometric hydroxyapatites promoted by Cobalt for the catalytic removal of oxygenated Volatile Organic Compounds. Catal. Lett. 135 (3–4), 197–206.
Akbayrak, S., Erdek, P., Özkar, S., 2013. Hydroxyapatite supported ruthenium(0) nanoparticles catalyst in hydrolytic dehydrogenation of ammonia borane: insight to the nanoparticles formation and hydrogen evolution kinetics. Appl. Catal. B Environ. 142–143, 187–195.
Anmin, H., Tong, L., Ming, L., Chengkang, C., Huiqin, L., Dali, M., 2006. Preparation of nanocrystals hydroxyapatite/TiO_2 compound by hydrothermal treatment. Appl. Catal. B Environ. 63 (1), 41–44.
Baba, A.A., Oduwole, I.T., Salami, F.O., Adekola, F.A., Adeboye, S.E., 2013. Synthesis of hydroxyapatite from waste egg-shell by Precipitation method. Ife J. Sci. 15 (3), 435–443.
Barbucci, R., 2007. Integrated Biomaterials Science. Springer Science & Business Media.
Bardhan, R., Mahata, S., Mondal, B., 2011. Processing of natural resourced hydroxyapatite from eggshell waste by wet precipitation method. Adv. Appl. Ceram. 110 (2), 80–86.
Barka, N., Qourzal, S., Assabbane, A., Nounah, A., Ait-Ichou, Y., 2011. Removal of Reactive Yellow 84 from aqueous solutions by adsorption onto hydroxyapatite. J. Saudi Chem. Soc. 15 (3), 263–267.
Barralet, J., Best, S., Bonfield, W., 1998. Carbonate substitution in precipitated hydroxyapatite: an investigation into the effects of reaction temperature and bicarbonate ion concentration. J. Biomed. Mater. Res. 41 (1), 79–86.
Bernardi, G., 1971a. Chromatography of proteins on hydroxyapatite. B.-M. in Enzymology, vol. 22. Ed. Academic Press, pp. 325–339.
Bernardi, G., 1971b. Chromatography of nucleic acids on hydroxyapatite columns. B.-M. in Enzymology, vol. 21. Ed. Academic Press, pp. 95–139.
Bernardi, G., 1973. Chromatography of proteins on hydroxyapatite. B.-M. in Enzymology, vol. 27. Ed. Academic Press, pp. 471–479.
Boechat, C.B., Eon, J.-G., Rossi, A.M., de Castro Perez, C.A., da S. San Gil, R.A., 2000. Structure of vanadate in calcium phosphate and vanadate apatite solid solutions. Phys. Chem. Chem. Phys. 2 (18), 4225–4230.
Boukha, Z., Kacimi, M., Ziyad, M., Ensuque, A., Bozon-Verduraz, F., 2007a. Comparative study of catalytic activity of Pd loaded hydroxyapatite and fluoroapatite in butan-2-ol conversion and methane oxidation. J. Mol. Catal. Chem. 270 (1), 205–213.
Boukha, Z., Kacimi, M., Pereira, M.F.R., Faria, J.L., Figueiredo, J.L., Ziyad, M., 2007b. Methane dry reforming on Ni loaded hydroxyapatite and fluoroapatite. Appl. Catal. A Gen. 317 (2), 299–309.
Boukha, Z., González-Prior, J., de Rivas, B., González-Velasco, J.R., López-Fonseca, R., Gutiérrez-Ortiz, J.I., 2016. Synthesis, characterisation and behaviour of Co/hydroxyapatite catalysts in the oxidation of 1,2-dichloroethane. Appl. Catal. B Environ. 190, 125–136.
Boukha, Z., Ayastuy, J.L., González-Velasco, J.R., Gutiérrez-Ortiz, M.A., 2017. CO elimination processes over promoter-free hydroxyapatite supported palladium catalysts. Appl. Catal. B Environ. 201, 189–201.
Boutinguiza, M., Pou, J., Comesaña, R., Lusquiños, F., De Carlos, A., León, B., 2012. Biological hydroxyapatite obtained from fish bones. Mater. Sci. Eng. C 32 (3), 478–486.
Brazón, E.M., Piccirillo, C., Moreira, I.S., Castro, P.M.L., 2016. Photodegradation of pharmaceutical persistent pollutants using hydroxyapatite-based materials. J. Environ. Manage. 182, 486–495.
Brunton, P.A., Davies, R.P.W., Burke, J.L., Smith, A., Aggeli, A., Brookes, S.J., Kirkham,

J., 2013. Treatment of early caries lesions using biomimetic self-assembling peptides–a clinical safety trial. Br. Dent. J. 215 (4) p. E6.
Buasri, A., Inkaew, T., Kodephun, L., Yenying, W., Loryuenyong, V., 2015. Natural hydroxyapatite (NHAp) derived from pork bone as a renewable catalyst for biodiesel production via microwave irradiation. Key Eng. Mater. 659, 216–220.
Cai, Y., Zhang, S., Zeng, X., Sun, D., 2011. Effect of fluorine incorporation on long-term stability of magnesium-containing hydroxyapatite coatings. J. Mater. Sci. Mater. Med. 22 (7), 1633–1638.
Campisi, S., Castellano, C., Gervasini, A., 2018. Tailoring the structural and morphological properties of hydroxyapatite materials to enhance the capture efficiency towards copper(II) and lead(II) ions. New J. Chem. 42 (6), 4520–4530.
Campisi, S., Galloni, M.G., Bossola, F., Gervasini, A., 2019. Comparative performance of copper and iron functionalized hydroxyapatite catalysts in NH_3-SCR. Catal. Commun. 123, 79–85.
Celik, D., Karahan, S., Zahmakıran, M., Özkar, S., 2012. Hydrogen generation from the hydrolysis of hydrazine-borane catalyzed by rhodium (0) nanoparticles supported on hydroxyapatite. Int. J. Hydrog. Energy 37 (6), 5143–5151.
Chai, Y., Tagaya, M., 2018. Simple preparation of hydroxyapatite nanostructures derived from fish scales. Mater. Lett. 222, 156–159.
Chai, Y., Ding, J., Wang, L., Liu, Q., Ren, J., Dai, W.-L., 2015. Enormous enhancement in photocatalytic performance of Ag_3PO_4/HAp composite: A Z-scheme mechanism insight. Appl. Catal. B Environ. 179, 29–36.
Chen, Y., Miao, X., 2005. Thermal and chemical stability of fluorohydroxyapatite ceramics with different fluorine contents. Biomaterials 26 (11), 1205–1210.
Chen, X., Wright, J.V., Conca, J.L., Peurrung, L.M., 1997a. Effects of pH on heavy metal sorption on mineral apatite. Environ. Sci. Technol. 31 (3), 624–631.
Chen, X., Wright, J.V., Conca, J.L., Peurrung, L.M., 1997b. Evaluation of heavy metal remediation using mineral apatite. Water Air Soil Pollut. 98 (1–2), 57–78.
Chen, S., Xu, M., Ma, Y., Yang, J., 2007. Evaluation of different phosphate amendments on availability of metals in contaminated soil. Ecotoxicol. Environ. Saf. 67 (2), 278–285.
Chlala, D., Labaki, M., Giraudon, J.-M., Gardoll, O., Denicourt-Nowicki, A., Roucoux, A., Lamonier, J.-F., 2016a. Toluene total oxidation over Pd and Au nanoparticles supported on hydroxyapatite. Comptes Rendus Chim. 19 (4), 525–537.
Chlala, D., Giraudon, J.-M., Nuns, N., Lancelot, C., Vannier, Rose-Noëlle, Labaki, M., Lamonier, J.-F., 2016b. Active Mn species well dispersed on Ca^{2+} enriched apatite for total oxidation of toluene. Appl. Catal. B Environ. 184, 87–95.
Coleman, S.J., Coronado, P.R., Maxwell, R.S., Reynolds, J.G., 2003. Granulated activated carbon modified with hydrophobic silica aerogel-potential composite materials for the removal of uranium from aqueous solutions. Environ. Sci. Technol. 37 (10), 2286–2290.
Condit, W., Hawley, E., Rectanus, H., Deeb, R., 2017. Global trends in the environmental remediation industry. J. Environ. Manage. 204, 705–708.
Corami, A., Mignardi, S., Ferrini, V., 2008. Cadmium removal from single- and multi-metal (Cd + Pb + Zn + Cu) solutions by sorption on hydroxyapatite. J. Colloid Interface Sci. 317 (2), 402–408.
Coulon, A., Grandjean, A., Laurencin, D., Jollivet, P., Rossignol, S., Campayo, L., 2017. Durability testing of an iodate-substituted hydroxyapatite designed for the conditioning of 129I. J. Nucl. Mater. 484, 324–331.
Cummings, L.J., Snyder, M.A., Brisack, K., 2009. Chapter 24 protein chromatography on hydroxyapatite columns. In: In: B, R.R., Deutscher, M.P. (Eds.), Methods in Enzymology 463. Ed. Academic Press, pp. 387–404.
De Araujo, T.S., De Souza, S.O., De Sousa, E.M.B., 2010. Effect of Zn^{2+}, Fe^{3+} and Cr^{3+} addition to hydroxyapatite for its application as an active constituent of sunscreens. J. Phys. Conf. Ser. 249 p. 012012.
del Rıo, J.G., Morando, P.J., Cicerone, D.S., 2004. Natural materials for treatment of industrial effluents: comparative study of the retention of Cd, Zn and Co by calcite and hydroxyapatite. Part I: batch experiments. J. Environ. Manage. 71 (2), 169–177.
Denry, I., Kuhn, L.T., 2016. Design and characterization of calcium phosphate ceramic scaffolds for bone tissue engineering. Dent. Mater. 32 (1), 43–53.
Diallo-Garcia, S., Osman, M.B., Krafft, J.-M., Casale, S., Thomas, C., Kubo, J., Costentin, G., 2014. Identification of surface basic sites and acid–base pairs of hydroxyapatite. J. Phys. Chem. C 118 (24), 12744–12757.
Domínguez, M.I., Romero-Sarria, F., Centeno, M.A., Odriozola, J.A., 2009. Gold/hydroxyapatite catalysts: synthesis, characterization and catalytic activity to CO oxidation. Appl. Catal. B Environ. 87 (3), 245–251.
Duff, E.J., 1972. Orthophosphates-XI bromoapatite: stability of solid solutions of bromoapatite with other calcium apatites under aqueous conditions. J. Inorg. Nucl. Chem. 34 (1), 101–108.
Dungkaew, W., Haller, K.J., Flood, A.E., Scamehorn, J.F., 2012. Arsenic removal by precipitation with Calcium phosphate hydroxyapatite. Adv. Mater. Res. 506, 413–416.
Durak, H., Gulcan, M., Zahmakiran, M., Ozkar, S., Kaya, M., 2014. Hydroxyapatite-nanosphere supported ruthenium (0) nanoparticle catalyst for hydrogen generation from ammonia-borane solution: kinetic studies for nanoparticle formation and hydrogen evolution. RSC Adv. 4 (55), 28947–28955.
El Asri, S., Laghzizil, A., Coradin, T., Saoiabi, A., Alaoui, A., M'hamedi, R., 2010. Conversion of natural phosphate rock into mesoporous hydroxyapatite for heavy metals removal from aqueous solution. Colloids Surf. Physicochem. Eng. Asp. 362 (1–3), 33–38.
El Azarifi, N., El Ouassouli, A., Lakhdar, M., Ezzamarty, A., Moreau, C., Travert, A., Leglise, J., 2005. Catalyst made of NiMo sulfide supported on hydroxyapatite: influence of Al addition on support properties and on the catalytic conversion of thiophene. J. Phys. IV France 123, 203–206.
El Bekkali, C., Bouyarmane, H., El Karbane, M., Masse, S., Saoiabi, A., Coradin, T., Laghzizil, A., 2018. Zinc oxide-hydroxyapatite nanocomposite photocatalysts for the degradation of ciprofloxacin and ofloxacin antibiotics. Colloids Surf. Physicochem. Eng. Asp. 539, 364–370.
El Idrissi, B., Yamni, K., Yacoubi, A., Massit, A., 2014. A novel method to synthesize nanocrystalline hydroxyapatite: characterization with X-ray diffraction and infrared spectroscopy. J Appl Chem 7, 107–112.
Elazarifi, N., Chaoui, M.A., El Ouassouli, A., Ezzamarty, A., Travert, A., Leglise, J., de Ménorval, L.-C., Moreau, C., 2004. Hydroprocessing of dibenzothiophene, 1-methylnaphthalene and quinoline over sulfided NiMo-hydroxyapatite-supported catalysts. Catal. Today 98 (no. 1), 161–170.
Elliot, J.C., 1994. Structure and Chemistry of the Apatites and Other Calcium Phosphates. Elsevier, Amsterdam.
Elliott, J.C., Young, R.A., 1967. Conversion of single crystals of chlorapatite into single crystals of hydroxyapatite. Nature 214 (5091), 904.
Elliott, J.C., Wilson, R.M., Dowker, S.E.P., 2002. Apatite structures. Adv. X-Ray Anal. 45, 172–181.
Epinette, J.-A., Manley, M.T., 2003. Fifteen Years of Clinical Experience With Hydroxyapatite Coatings in Joint Arthroplasty. Springer Science & Business Media.
Eslami, H., Solati-Hashjin, M., Tahriri, M., 2008. Synthesis and characterization of nanocrystalline fluorinated hydroxyapatite powder by modified wet-chemical process. J. Ceram. Process Res. 9, 224–229.
Fan, X., Parker, D.J., Smith, M.D., 2003. Adsorption kinetics of fluoride on low cost materials. Water Res. 37 (20), 4929–4937.
Fang, Y., Agrawal, D.K., Roy, D.M., 1994. Thermal stability of synthetic hydroxyapatite. In: Brown, P.W., Constantz, B. (Eds.), Hydroxyapatite and Related Materials. CRC Press.
Farooq, M., Ramli, A., Naeem, A., 2015. Biodiesel production from low FFA waste cooking oil using heterogeneous catalyst derived from chicken bones. Renew. Energy 76, 362–368.
Feng, Y., Gong, J.-L., Zeng, G.-M., Niu, Q.-Y., Zhang, H.-Y., Niu, C.-G., Deng, J.-H., Yan, M., 2010. Adsorption of Cd (II) and Zn (II) from aqueous solutions using magnetic hydroxyapatite nanoparticles as adsorbents. Chem. Eng. J. 162 (2), 487–494.
Ferri, M., Campisi, S., Scavini, M., Evangelisti, C., Carniti, P., Gervasini, A., 2019. In-depth study of the mechanism of heavy metal trapping on the surface of hydroxyapatite. Appl. Surf. Sci. 475, 397–409.
Fihri, A., Len, C., Varma, R.S., Solhy, A., 2017. Hydroxyapatite: a review of syntheses, structure and applications in heterogeneous catalysis. Coord. Chem. Rev. 347, 48–76.
Fleet, M.E., Liu, X., 2007. Coupled substitution of type A and B carbonate in sodium-bearing apatite. Biomaterials 28 (6), 916–926.
Fleet, M.E., Liu, X., King, P.L., 2004. Accommodation of the carbonate ion in apatite: an FTIR and X-ray structure study of crystals synthesized at 2–4 GPa. Am. Mineral. 89 (10), 1422–1432.
Flores-Cano, J.V., Leyva-Ramos, R., Carrasco-Marin, F., Aragón-Piña, A., Salazar-Rabago, J.J., Leyva-Ramos, S., 2016. Adsorption mechanism of Chromium(III) from water solution on bone char: effect of operating conditions. Adsorption 22 (3), 297–308.
Fu, H., Rahaman, M.N., Brown, R.F., Day, D.E., 2013. Evaluation of BSA protein release from hollow hydroxyapatite microspheres into PEG hydrogel. Mater. Sci. Eng. C 33 (4), 2245–2250.
Fu, L.-H., Liu, Y.-J., Ma, M.-G., Zhang, X.-M., Xue, Z.-M., Zhu, J.-F., 2016. Microwave-assisted hydrothermal synthesis of cellulose/hydroxyapatite nanocomposites. Polymers 8 (9), 316.
Fuller, C.C., Bargar, J.R., Davis, J.A., Piana, M.J., 2002. Mechanisms of uranium interactions with hydroxyapatite: implications for groundwater remediation. Environ. Sci. Technol. 36 (2), 158–165.
Gao, S., Sun, R., Wei, Z., Zhao, H., Li, H., Hu, F., 2009a. Size-dependent defluoridation properties of synthetic hydroxyapatite. J. Fluor. Chem. 130 (6), 550–556.
Gao, S., Cui, J., Wei, Z., 2009b. Study on the fluoride adsorption of various apatite materials in aqueous solution. J. Fluor. Chem. 130 (11), 1035–1041.
Giannakopoulou, T., Todorova, N., Romanos, G., Vaimakis, T., Dillert, R., Bahnemann, D., Trapalis, C., 2012. Composite hydroxyapatite/TiO_2 materials for photocatalytic oxidation of NO_x. Mater. Sci. Eng. B 177 (13), 1046–1052.
Gibson, I.R., Bonfield, W., 2002. Novel synthesis and characterization of an AB-type carbonate-substituted hydroxyapatite. J. Biomed. Mater. Res. 59 (4), 697–708.
Gibson, I.R., Best, S.M., Bonfield, W., 1999. Chemical characterization of silicon-substituted hydroxyapatite. J. Biomed. Mater. Res. A 44 (no. 4), 422–428.
Green, D.J., 1998. An Introduction to the Mechanical Properties of Ceramics. Cambridge University Press.
Gupta, J., Agarwal, M., 2017. Biodiesel production from a mixture of vegetable oils using marble slurry derived heterogeneous catalyst. Curr. Trends Biomed. Eng. Biosci. 5 (1).
Gupta, J., Agarwal, M., Dalai, A.K., 2018. Marble slurry derived hydroxyapatite as heterogeneous catalyst for biodiesel production from soybean oil. Can. J. Chem. Eng. 96 (9), 1873–1880.
Haberko, K., Bućko, M.M., Brzezińska-Miecznik, J., Haberko, M., Mozgawa, W., Panz, T., Pyda, A., Zarębski, J., 2006. Natural hydroxyapatite—its behaviour during heat treatment. J. Eur. Ceram. Soc. 26 (4–5), 537–542.
Hadioui, M., Sharrock, P., Mecherri, M.-O., Brumas, V., Fiallo, M., 2008. Reaction of lead ions with hydroxylapatite granules. Chem. Pap. 62 (5), 516–521.
Haider, A., Haider, S., Han, S.S., Kang, I.-K., 2017. Recent advances in the synthesis, functionalization and biomedical applications of hydroxyapatite: a review. RSC Adv. 7 (13), 7442–7458.
Han, H., Qian, X., Yuan, Y., Zhou, M., Chen, Y., 2016. Photocatalytic degradation of dyes in water using TiO_2/Hydroxyapatite composites. Water Air Soil Pollut. 227 (12), 461.
Hasan, M.A., Moore, R.C., Holt, K.C., Hasan, A.A., 2003. Overview on Backfill Materials and Permeable Reactive Barriers for Nuclear Waste Disposal Facilities. Sandia Natl. Lab., New México USA, pp. 1–27.
Hidouri, M., Bouzouita, K., Kooli, F., Khattech, I., 2003. Thermal behaviour of

magnesium-containing fluorapatite. Mater. Chem. Phys. 80 (2), 496–505.
Holkar, C.R., Jadhav, A.J., Pinjari, D.V., Mahamuni, N.M., Pandit, A.B., 2016. A critical review on textile wastewater treatments: possible approaches. J. Environ. Manage. 182, 351–366.
Hu, C., Guo, J., Qu, J., Hu, X., 2007. Efficient destruction of bacteria with Ti(IV) and antibacterial ions in co-substituted hydroxyapatite films. Appl. Catal. B Environ. 73 (3), 345–353.
Hu, M., Yao, Z., Liu, X., Ma, L., He, Z., Wang, X., 2018. Enhancement mechanism of hydroxyapatite for photocatalytic degradation of gaseous formaldehyde over TiO_2/hydroxyapatite. J. Taiwan Inst. Chem. Eng. 85, 91–97.
Huang, J., Wang, L.-C., Liu, Y.-M., Cao, Y., He, H.-Y., Fan, K.-N., 2011. Gold nanoparticles supported on hydroxylapatite as high performance catalysts for low temperature CO oxidation. Appl. Catal. B Environ. 101 (3), 560–569.
Huang, C., Ma, Z., Xie, P., Yue, Y., Hua, W., Gao, Z., 2015. Hydroxyapatite-supported rhodium catalysts for N_2O decomposition. J. Mol. Catal. Chem. 400, 90–94.
Huang, C., Jiang, Y., Ma, Z., Xie, P., Lin, Y., Meng, T., Miao, C., Yue, Y., Hua, W., Gao, Z., 2016. Correlation among preparation methods/conditions, physicochemical properties, and catalytic performance of Rh/hydroxyapatite catalysts in N_2O decomposition. J. Mol. Catal. Chem. 420, 73–81.
Ioku, K., 2010. Tailored bioceramics of calcium phosphates for regenerative medicine. J. Ceram. Soc. Jpn. 118 (1381), 775–783.
Ishikawa, K., Ducheyne, P., Radin, S., 1993. Determination of the Ca/P ratio in calcium-deficient hydroxyapatite using X-ray diffraction analysis. J. Mater. Sci. Mater. Med. 4 (2), 165–168.
Itagaki, T., Yoshida, M., Abe, S., Omichi, H., Nishihira, Y., 1993. Separation of human tear proteins with ceramic hydroxyapatite high-performance liquid chromatography. J. Chromatogr. B. Biomed. Sci. App. 620 (1), 149–152.
Jaworski, J.W., Cho, S., Kim, Y., Jung, J.H., Jeon, H.S., Min, B.K., Kwon, K.-Y., 2013. Hydroxyapatite supported cobalt catalysts for hydrogen generation. J. Colloid Interface Sci. 394, 401–408.
Jemal, J., Tounsi, H., Chaari, K., Petitto, C., Delahay, G., Djemel, S., Ghorbel, A., 2012. NO reduction with NH_3 under oxidizing atmosphere on copper loaded hydroxyapatite. Appl. Catal. B Environ. 113, 255–260.
Ji, S., Murakami, S., Kamitakahara, M., Ioku, K., 2009. Fabrication of titania/hydroxyapatite composite granules for photo-catalyst. Mater. Res. Bull. 44 (4), 768–774.
Jones, M.I., Barakat, H., Patterson, D.A., 2011. Production of hydroxyapatite from waste mussel shells. IOP Conference Series: Materials Science and Engineering, vol. 18 pp. 192002.
Joschek, S., Nies, B., Krotz, R., Göpferich, A., 2000. Chemical and physicochemical characterization of porous hydroxyapatite ceramics made of natural bone. Biomaterials 21 (16), 1645–1658.
Jun, J.H., Lee, T.-J., Lim, T.H., Nam, S.-W., Hong, S.-A., Yoon, K.J., 2004. Nickel–calcium phosphate/hydroxyapatite catalysts for partial oxidation of methane to syngas: characterization and activation. J. Catal. 221 (1), 178–190.
Kadoya, T., 1990. High-performance liquid chromatography of proteins on a ceramic hydroxyapatite with volatile buffers. J. Chromatogr. A 515, 521–525.
Kaluđerović Radoičić, T., Raičević, S., 2008. In situ lead stabilization using natural and synthetic apatite. Chem. Ind. Chem. Eng. Q. 14 (4), 269–271.
Kanchana, P., Sekar, C., 2010. Influence of sodium fluoride on the synthesis of hydroxyapatite by gel method. J. Cryst. Growth 312 (6), 808–816.
Kandori, K., Mizumoto, S., Toshima, S., Fukusumi, M., Morisada, Y., 2009. Effects of heat treatment of calcium hydroxyapatite particles on the protein adsorption behavior. J. Phys. Chem. B 113 (31), 11016–11022.
Kandori, K., Toshima, S., Wakamura, M., Fukusumi, M., Morisada, Y., 2010. Effects of modification of calcium hydroxyapatites by trivalent metal ions on the protein adsorption behavior. J. Phys. Chem. B 114 (7), 2399–2404.
Kapoor, S., Batra, U., Suchita, K., 2016. Investigation on influence of fluorine substitution on structural, thermal and in-vitro behaviour of nanodimensional hydroxyapatite. J. Chem. Pharm. Res. 8 (3), 281–288.
Karamian, E., Abdellahi, M., Khandan, A., Abdellah, S., 2016. Introducing the fluorine doped natural hydroxyapatite-titania nanobiocomposite ceramic. J. Alloys Compd. 679, 375–383.
Kawasaki, T., Takahashi, S., Ideda, K., 1985. Hydroxyapatite high-performance liquid chromatography: column performance for proteins. Eur. J. Biochem. 152 (2), 361–371.
Khachani, M., Kacimi, M., Ensuque, A., Piquemal, J.-Y., Connan, C., Bozon-Verduraz, F., Ziyad, M., 2010. Iron–calcium–hydroxyapatite catalysts: iron speciation and comparative performances in butan-2-ol conversion and propane oxidative dehydrogenation. Appl. Catal. A Gen. 388 (1), 113–123.
Kibby, C.L., Hall, W.K., 1973. Dehydrogenation of alcohols and hydrogen transfer from alcohols to ketones over hydroxyapatite catalysts. J. Catal. 31 (1), 65–73.
Kim, H.-W., Kim, H.-E., Knowles, J.C., 2004. Fluor-hydroxyapatite sol–gel coating on titanium substrate for hard tissue implants. Biomaterials 25 (17), 3351–3358.
Kongsri, S., Janpradit, K., Buapa, K., Techawongstien, S., Chanthai, S., 2013. Nanocrystalline hydroxyapatite from fish scale waste: preparation, characterization and application for selenium adsorption in aqueous solution. Chem. Eng. J. 215, 522–532.
Kumar, P.A., Reddy, M.P., Ju, L.K., Phil, H.H., 2008. Novel silver loaded hydroxyapatite catalyst for the selective catalytic reduction of NO_x by propene. Catal. Lett. 126 (1–2), 78–83.
Kumari, M., Saroha, A.K., 2018. Performance of various catalysts on treatment of refractory pollutants in industrial wastewater by catalytic wet air oxidation: a review. J. Environ. Manage. 228, 169–188.
Kuśnieruk, S., Wojnarowicz, J., Chodara, A., Chudoba, T., Gierlotka, S., Lojkowski, W., 2016. Influence of hydrothermal synthesis parameters on the properties of hydroxyapatite nanoparticles. Beilstein J. Nanotechnol. 7 (1), 1586–1601.
Lafon, J.-P., Champion, E., Bernache-Assollant, D., 2008. Processing of AB-type carbonated hydroxyapatite $Ca_{10-x}(PO_4)_{6-x}(CO_3)_x(OH)_{2-x-2y}(CO_3)_y$ ceramics with controlled composition. J. Eur. Ceram. Soc. 28 (1), 139–147.
Lamonier, C., Lamonier, J.-F., Aellach, B., Ezzamarty, A., Leglise, J., 2011. Specific tuning of acid/base sites in apatite materials to enhance their methanol thiolation catalytic performances. Catal. Today 164 (1), 124–130.
Laurencin, D., Almora-Barrios, N., de Leeuw, N.H., Gervais, C., Bonhomme, C., Mauri, F., Chrzanowski, W., Knowles, J.C., Newport, R.J., Wong, A., 2011. Magnesium incorporation into hydroxyapatite. Biomaterials 32 (7), 1826–1837.
Lee, S.J., Jun, J.H., Lee, S.-H., Yoon, K.J., Lim, T.H., Nam, S.-W., Hong, S.-A., 2002. Partial oxidation of methane over nickel-added strontium phosphate. Appl. Catal. A Gen. 230 (1), 61–71.
Lee, E.-J., Lee, S.-H., Kim, H.-W., Kong, Y.-M., Kim, H.-E., 2005a. Fluoridated apatite coatings on titanium obtained by electron-beam deposition. Biomaterials 26 (18), 3843–3851.
Lee, C.-K., Kim, H.-S., Kwon, J.-H., Lee, C.-K., Kim, H.-S., Kwon, J.-H., 2005b. The removal of heavy metals using hydroxyapatite. Environ. Eng. Res. 10 (5), 205–212.
LeGeros, R.Z., Legeros, J.P., 1984. Phosphate minerals in human tissues. Phosphate Minerals. Springer, pp. 351–385.
Leventouri, T., 2006. Synthetic and biological hydroxyapatites: crystal structure questions. Biomaterials 27 (18), 3339–3342.
Li, Y., Ho, J., Ooi, C.P., 2010. Antibacterial efficacy and cytotoxicity studies of copper (II) and titanium (IV) substituted hydroxyapatite nanoparticles. Mater. Sci. Eng. C 30 (8), 1137–1144.
Li, R., Chen, K., Li, G., Han, G., Yu, S., Yao, J., Cai, Y., 2016. Structure design and fabrication of porous hydroxyapatite microspheres for cell delivery. J. Mol. Struct. 1120, 34–41.
Lin, K., Pan, J., Chen, Y., Cheng, R., Xu, X., 2009. Study the adsorption of phenol from aqueous solution on hydroxyapatite nanopowders. J. Hazard. Mater. 161 (1), 231–240.
Lin, Y., Meng, T., Ma, Z., 2015. Catalytic decomposition of N_2O over RhO_x supported on metal phosphates. J. Ind. Eng. Chem. 28, 138–146.
Liu, Y., Peng, Y., 2015. Advanced Material Engineering: Proceedings of the 2015 International Conference on Advanced Material Engineering. World Scientific.
Liu, G., Talley, J.W., Na, C., Larson, S.L., Wolfe, L.G., 2010. Copper doping improves hydroxyapatite sorption for arsenate in simulated groundwaters. Environ. Sci. Technol. 44 (4), 1366–1372.
Liu, X., Ma, J., Yang, J., 2014. Visible-light-driven amorphous Fe(III)-substituted hydroxyapatite photocatalyst: characterization and photocatalytic activity. Mater. Lett. 137, 256–259.
Liu, W., Qian, G., Zhang, B., Liu, L., Liu, H., 2016. Facile synthesis of spherical nano hydroxyapatite and its application in photocatalytic degradation of methyl orange dye under UV irradiation. Mater. Lett. 178, 15–17.
Ma, Q.Y., Traina, S.J., Logan, T.J., Ryan, J.A., 1993. In situ lead immobilization by apatite. Env. Sci. Technol. 27 (9), 1803–1810.
Ma, Q.Y., Traina, S.J., Logan, T.J., Ryan, J.A., 1994a. Effects of aqueous Al, Cd, Cu, Fe (II), Ni, and Zn on Pb immobilization by hydroxyapatite. Environ. Sci. Technol. 28 (7), 1219–1228.
Ma, Q.Y., Logan, T.J., Traina, S.J., Ryan, J.A., 1994b. Effects of NO_3^-, Cl^-, F^-, SO_4^{2-}, and CO_3^{2-} on Pb^{2+} immobilization by hydroxyapatite. Environ. Sci. Technol. 28 (3), 408–418.
Mahapatra, P.P., Mahapatra, L.M., Mishra, B., 1989. Physicochemical studies on solid solutions of calcium phosphorus arsenic hydroxyapatites. Bull. Chem. Soc. Jpn. 62 (10), 3272–3277.
Malina, D., Biernat, K., Sobczak-Kupiec, A., 2013. Studies on sintering process of synthetic hydroxyapatite. Acta Biochim. Pol. 60 (4), 851–855.
Masuyama, Y., Yoshikawa, K., Suzuki, N., Hara, K., Fukuoka, A., 2011. Hydroxyapatite-supported copper(II)-catalyzed azide–alkyne [3 + 2] cycloaddition with neither reducing agents nor bases in water. Tetrahedron Lett. 52 (51), 6916–6918.
Matsuda, T., Yamanaka, C., Ikeya, M., 2005. ESR study of Gd^{3+} and Mn^{2+} ions sorbed on hydroxyapatite. Appl. Radiat. Isot. 62 (2), 353–357.
Matsumura, Y., Sugiyama, S., Hayashi, H., Shigemota, N., Saitoh, K., Moffat, J.B., 1994. Strontium hydroxyapatites: catalytic properties in the oxidative dehydrogenation of methane to carbon oxides and hydrogen. J. Mol. Catal. 92 (1), 81–94.
Matsunaga, K., Murata, H., Mizoguchi, T., Nakahira, A., 2010. Mechanism of incorporation of zinc into hydroxyapatite. Acta Biomater. 6 (6), 2289–2293.
Meza, D., Figueroa, I.A., Flores-Morales, C., Piña-Barba, M.C., 2011. Nano hydroxyapatite crystals obtained by colloidal solution. Rev. Mex. Física 57 (6), 471–474.
Mitsionis, A., Vaimakis, T., Trapalis, C., Todorova, N., Bahnemann, D., Dillert, R., 2011. Hydroxyapatite/titanium dioxide nanocomposites for controlled photocatalytic NO oxidation. Appl. Catal. B Environ. 106 (3), 398–404.
Mobasherpour, I., Salahi, E., Pazouki, M., 2011. Removal of nickel (II) from aqueous solutions by using nano-crystalline calcium hydroxyapatite. J. Saudi Chem. Soc. 15 (2), 105–112.
Mobasherpour, I., Salahi, E., Pazouki, M., 2012. Comparative of the removal of Pb^{2+}, Cd^{2+} and Ni^{2+} by nano crystallite hydroxyapatite from aqueous solutions: Adsorption isotherm study. Arab. J. Chem. 5 (4), 439–446.
Mondal, S., Pal, U., Dey, A., 2016a. Natural origin hydroxyapatite scaffold as potential bone tissue engineering substitute. Ceram. Int. 42 (16), 18338–18346.
Mondal, B., Mondal, S., Mondal, A., Mandal, N., 2016b. Fish scale derived hydroxyapatite scaffold for bone tissue engineering. Mater. Charact. 121, 112–124.
Mondal, S., Dorozhkin, S.V., Pal, U., 2018. Recent progress on fabrication and drug delivery applications of nanostructured hydroxyapatite. Wiley Interdiscip. Rev. Nanomed. Nanobiotechnol. 10 (4), e1504.
Monteil-Rivera, F., Fedoroff, M., Jeanjean, J., Minel, L., Barthes, M.-G., Dumonceau, J., 2000. Sorption of selenite (SeO_3^{2-}) on hydroxyapatite: an exchange process. J.

Colloid Interface Sci. 221 (2), 291–300.
Mourabet, M., El Rhilassi, A., El Boujaady, H., Bennani-Ziatni, M., El Hamri, R., Taitai, A., 2015. Removal of fluoride from aqueous solution by adsorption on hydroxyapatite (HAp) using response surface methodology. J. Saudi Chem. Soc. 19 (6), 603–615.
Mousa, S.M., Ammar, N.S., Ibrahim, H.A., 2016. Removal of lead ions using hydroxyapatite nano-material prepared from phosphogypsum waste. J. Saudi Chem. Soc. 20 (3), 357–365.
Muhammad, N., Gao, Y., Iqbal, F., Ahmad, P., Ge, R., Nishan, U., Rahim, A., Gonfa, G., Ullah, Z., 2016. Extraction of biocompatible hydroxyapatite from fish scales using novel approach of ionic liquid pretreatment. Sep. Purif. Technol. 161, 129–135.
Murgolo, S., Moreira, I., Piccirillo, M., Castro, P., Ventrella, G., Cocozza, C., Mascolo, G., 2018. Photocatalytic Degradation of Diclofenac by Hydroxyapatite–TiO_2 Composite Material: Identification of Transformation Products and Assessment of Toxicity. Materials 11 (9), 1779.
Nasiri-Tabrizi, B., Fahami, A., Ebrahimi, F., Ebrahimi-Kahrizsangi, R., 2012. New Frontiers in Mechanosynthesis: Hydroxyapatite-and Fluorapatite-Based Nanocomposite Powders. INTECH Open Access Publisher.
Nilen, R.W.N., Richter, P.W., 2008. The thermal stability of hydroxyapatite in biphasic calcium phosphate ceramics. J. Mater. Sci. Mater. Med. 19 (4), 1693–1702.
Nishikawa, H., 2003. Surface changes and radical formation on hydroxyapatite by UV irradiation for inducing photocatalytic activation. J. Mol. Catal. Chem. 206 (1), 331–338.
Nishikawa, H., 2004a. A high active type of hydroxyapatite for photocatalytic decomposition of dimethyl sulfide under UV irradiation. J. Mol. Catal. Chem. 207 (2), 149–153.
Nishikawa, H., 2004b. Photocatalytic activity of hydroxyapatite based on photo-induced excitation. Phosphorus Res. Bull. 17, 101–104.
Nishikawa, H., Monma, H., 1993. Vapor phase decomposition with dechlorination of organic chlorinated compounds over calcium-deficient hydroxyapatite. Phosphorus Res. Bull. 3, 115–118.
Nishikawa, H., Monma, H., 1994. Oxidative decomposition of chlorobenzene over calcium-deficient hydroxyapatite. Bull. Chem. Soc. Jpn. 67 (9), 2454–2456.
Nishikawa, H., Ikeda, S., Monma, H., 1993. Characterization of calcium-deficient hydroxyapatite after a catalytic reaction with trichloroethylene vapor. Bull. Chem. Soc. Jpn. 66 (9), 2570–2573.
Nishikawa, H., Oka, T., Asai, N., Simomichi, H., Shirai, T., Fuji, M., 2012. Oxidative decomposition of volatile organic compounds using thermally-excited activity of hydroxyapatite. Appl. Surf. Sci. 258 (14), 5370–5374.
Obadiah, A., Swaroopa, G.A., Kumar, S.V., Jeganathan, K.R., Ramasubbu, A., 2012. Biodiesel production from palm oil using calcined waste animal bone as catalyst. Bioresour. Technol. 116, 512–516.
Og, O., Fa, A., 2018. Removal of Iron and manganese from aqueous solution using hydroxyapatite prepared from cow bone. Res. Rev. J. Mater. Sci. 6 (2), 59–72.
Oh, S.C., Wu, Y., Tran, D.T., Lee, I.C., Lei, Y., Liu, D., 2016. Influences of cation and anion substitutions on oxidative coupling of methane over hydroxyapatite catalysts. Fuel 167, 208–217.
Oh, S.C., Lei, Y., Chen, H., Liu, D., 2017. Catalytic consequences of cation and anion substitutions on rate and mechanism of oxidative coupling of methane over hydroxyapatite catalysts. Fuel 191, 472–485.
Ooi, C.Y., Hamdi, M., Ramesh, S., 2007. Properties of hydroxyapatite produced by annealing of bovine bone. Ceram. Int. 33 (7), 1171–1177.
Opre, Z., 2007. Catalytic Oxidation Over Transition Metal Containing Hydroxyapatites. PhD Thesis. ETH Zurich.
Opre, Z., Grunwaldt, J.-D., Maciejewski, M., Ferri, D., Mallat, T., Baiker, A., 2005. Promoted Ru–hydroxyapatite: designed structure for the fast and highly selective oxidation of alcohols with oxygen. J. Catal. 230 (2), 406–419.
Orlovskii, V.P., Komlev, V.S., Barinov, S.M., 2002. Hydroxyapatite and hydroxyapatite-based ceramics. Inorg. Mater. 38 (10), 973–984.
Özhava, D., Özkar, S., 2015. Rhodium(0) nanoparticles supported on hydroxyapatite nanospheres and further stabilized by dihydrogen phosphate ion: a highly active catalyst in hydrogen generation from the methanolysis of ammonia borane. Int. J. Hydrog. Energy 40 (33), 10491–10501.
Pal, A., Paul, S., Choudhury, A.R., Balla, V.K., Das, M., Sinha, A., 2017. Synthesis of hydroxyapatite from Lates calcarifer fish bone for biomedical applications. Mater. Lett. 203, 89–92.
Palazzo, B., Sidoti, M.C., Roveri, N., Tampieri, A., Sandri, M., Bertolazzi, L., Galbusera, F., Dubini, G., Vena, P., Contro, R., 2005. Controlled drug delivery from porous hydroxyapatite grafts: an experimental and theoretical approach. Mater. Sci. Eng. C 25 (2), 207–213.
Park, J., Lakes, R.S., 2007. Biomaterials: An Introduction. Springer Science & Business Media.
Pasteris, J.D., 2012. Structurally incorporated water in bone apatite: a cautionary tale. In: Heimann, R.B. (Ed.), Calcium Phosphates: Structure, Synthesis, Properties, and Applications. Nova Science Publishers, Inc., Ed. New York, pp. 63–94.
Phonthammachai, N., Ziyi, Z., Jun, G., Fan, H.Y., Whitea, T.J., 2008. Synthesis of high performance hydroxyapatite-gold catalysts for CO oxidation. Gold Bull. 41 (1), 42–50.
Piccirillo, C., Pullar, R.C., Tobaldi, D.M., Castro, P.L., Pintado, M.E., 2014. Hydroxyapatite and chloroapatite derived from sardine by-products. Ceram. Int. 40 (8), 13231–13240.
Piccirillo, C., Denis, C.J., Pullar, R.C., Binions, R., Parkin, I.P., Darr, J.A., Castro, P.M.L., 2017. Aerosol assisted chemical vapour deposition of hydroxyapatite-embedded titanium dioxide composite thin films. J. Photochem. Photobiol. Chem. 332, 45–53.
Poinern, G.E.J., Ghosh, M.K., Ng, Y.-J., Issa, T.B., Anand, S., Singh, P., 2011. Defluoridation behavior of nanostructured hydroxyapatite synthesized through an ultrasonic and microwave combined technique. J. Hazard. Mater. 185 (1), 29–37.
Pon-On, W., Suntornsaratoon, P., Charoenphandhu, N., Thongbunchoo, J., Krishnamra, N., Tang, I.M., 2016. Hydroxyapatite from fish scale for potential use as bone scaffold or regenerative material. Mater. Sci. Eng. C 62, 183–189.
Prakasam, M., Locs, J., Salma-Ancane, K., Loca, D., Largeteau, A., Berzina-Cimdina, L., 2015. Fabrication, properties and applications of dense hydroxyapatite: a review. J. Funct. Biomater. 6 (4), 1099–1140.
Prasad, M., Xu, H., Saxena, S., 2008. Multi-component sorption of Pb (II), Cu (II) and Zn (II) onto low-cost mineral adsorbent. J. Hazard. Mater. 154 (1–3), 221–229.
Pratap Reddy, M., Venugopal, A., Subrahmanyam, M., 2007. Hydroxyapatite-supported Ag–TiO_2 as Escherichia coli disinfection photocatalyst. Water Res. 41 (2), 379–386.
Prener, J.S., 1967. The growth and crystallographic properties of calcium fluor-and chlorapatite crystals. J. Electrochem. Soc. 114 (1), 77–83.
Qu, Z., Sun, Y., Chen, D., Wang, Y., 2014. Possible sites of copper located on hydroxyapatite structure and the identification of active sites for formaldehyde oxidation. J. Mol. Catal. Chem. 393, 182–190.
Rajesh, R., Hariharasubramanian, A., Ravichandran, Y.D., 2012. Chicken bone as a bioresource for the bioceramic (Hydroxyapatite). Phosphorus Sulfur Silicon Relat. Elem. 187 (8), 914–925.
Rakap, M., Özkar, S., 2011. Hydroxyapatite-supported palladium(0) nanoclusters as effective and reusable catalyst for hydrogen generation from the hydrolysis of ammonia-borane. Int. J. Hydrog. Energy 36 (12), 7019–7027.
Rakap, M., Özkar, S., 2012. Hydroxyapatite-supported cobalt(0) nanoclusters as efficient and cost-effective catalyst for hydrogen generation from the hydrolysis of both sodium borohydride and ammonia-borane. Catal. Today 183 (1), 17–25.
Reddy, M.P., Venugopal, A., Subrahmanyam, M., 2007. Hydroxyapatite photocatalytic degradation of calmagite (an azo dye) in aqueous suspension. Appl. Catal. B Environ. 69 (3–4), 164–170.
Rêgo De Vasconcelos, B., Zhao, L., Sharrock, P., Nzihou, A., Pham Minh, D., 2016. Catalytic transformation of carbon dioxide and methane into syngas over ruthenium and platinum supported hydroxyapatites. Appl. Surf. Sci. 390, 141–156.
Reichert, J., Binner, J.G.P., 1996. An evaluation of hydroxyapatite-based filters for removal of heavy metal ions from aqueous solutions. J. Mater. Sci. 31 (5), 1231–1241.
Resende, N.S., Nele, M., Salim, V.M., 2006. Effects of anion substitution on the acid properties of hydroxyapatite. Thermochim. Acta 451 (1), 16–21.
Riad, M., Mikhail, S., 2012. Oxidative desulfurization of light gas oil using zinc catalysts prepared via different techniques. Catal. Sci. Technol. 2 (7), 1437–1446.
Ribeiro Alves, M.R., Zuñiga, A.D.G., de Sousa, R.C.S., Zacchi Scolforo, C., 2016. The process of separating bovine serum albumin using hydroxyapatite and active babassu coal (Orbignya martiana). Sci. World J. 2016 9 pages.
Rigali, M.J., Brady, P.V., Moore, R.C., 2016. Radionuclide removal by apatite. Am. Mineral. 101 (12), 2611–2619.
Rulis, P., Ouyang, L., Ching, W.Y., 2004. Electronic structure and bonding in calcium apatite crystals: hydroxyapatite, fluorapatite, chlorapatite, and bromapatite. Phys. Rev. B 70 (15), 155104.
Sahibed-dine, A., Bentiss, F., Bensitel, M., 2017. The photocatalytic degradation of methylene bleu over TiO_2 catalysts supported on hydroxyapatite. J. Mater. 8 (4), 1301–1311.
Salma, K., Berzina-Cimdina, L., Borodajenko, N., 2010. Calcium phosphate bioceramics prepared from wet chemically precipitated powders. Process. Appl. Ceram. 4 (1), 45–51.
Sasaki, K., Goto, T., 2014. Immobilization of Sr^{2+} on naturally derived hydroxyapatite by calcination of different species of fish bones and influence of calcination on ion-exchange efficiency. Ceram. Int. 40 (8), 11649–11656.
Savaris, D.L., de Matos, R., Lindino, C.A., 2018. Degradation of 17α-methyltestosterone by hydroxyapatite catalyst. Rev. Ambiente Água 13 (1).
Schiavoni, M., Campisi, S., Carniti, P., Gervasini, A., Delplanche, T., 2018. Focus on the catalytic performances of Cu-functionalized hydroxyapatites in NH_3-SCR reaction. Appl. Catal. A Gen. 563, 43–53.
Shaaban, M., Van Zwieten, L., Bashir, S., Younas, A., Núñez-Delgado, A., Chhajro, M., Kubar, K.A., Ali, U., Rana, M.S., Mehmood, M.A., 2018. A concise review of biochar application to agricultural soils to improve soil conditions and fight pollution. J. Environ. Manage. 228, 429–440.
Shariffuddin, J.H., Jones, M.I., Patterson, D.A., 2013. Greener photocatalysts: hydroxyapatite derived from waste mussel shells for the photocatalytic degradation of a model azo dye wastewater. Chem. Eng. Res. Des. 91 (9), 1693–1704.
Silva, G.C., Ma, L., Hemmers, O., Lindle, D., 2008. Micro-structural characterization of precipitation-synthesized fluorapatite nano-material by transmission electron microscopy using different sample preparation techniques. Micron 39 (3), 269–274.
Silvester, L., Lamonier, J.-F., Vannier, R.-N., Lamonier, C., Capron, M., Mamede, A.-S., Pourpoint, F., Gervasini, A., Dumeignil, F., 2014. Structural, textural and acid–base properties of carbonate-containing hydroxyapatites. J. Mater. Chem. A 2 (29), 11073–11090.
Silvester, L., Lamonier, J.-F., Faye, J., Capron, M., Vannier, R.-N., Lamonier, C., Dubois, J.-L., Couturier, J.-L., Calais, C., Dumeignil, F., 2015. Reactivity of ethanol over hydroxyapatite-based Ca-enriched catalysts with various carbonate contents. Catal. Sci. Technol. 5 (5), 2994–3006.
Smičiklas, I.D., Milonjić, S.K., Pfendt, P., Raičević, S., 2000. The point of zero charge and sorption of cadmium (II) and strontium (II) ions on synthetic hydroxyapatite. Sep. Purif. Technol. 18 (3), 185–194.
Smith, S.M., Oopathum, C., Weeramongkhonlert, V., Smith, C.B., Chaveanghong, S., Ketwong, P., Boonyuen, S., 2013. Transesterification of soybean oil using bovine bone waste as new catalyst. Bioresour. Technol. 143, 686–690.
Son, J.S., Appleford, M., Ong, J.L., Wenke, J.C., Kim, J.M., Choi, S.H., Oh, D.S., 2011. Porous hydroxyapatite scaffold with three-dimensional localized drug delivery system using biodegradable microspheres. J. Control. Release 153 (2), 133–140.
Sopyan, I., Mel, M., Ramesh, S., Khalid, K.A., 2007. Porous hydroxyapatite for artificial

bone applications. Sci. Technol. Adv. Mater. 8 (1), 116–123.
Srinivasan, M., Ferraris, C., White, T., 2006. Cadmium and lead ion capture with three dimensionally ordered macroporous hydroxyapatite. Environ. Sci. Technol. 40 (22), 7054–7059.
Stötzel, C., Müller, F.A., Reinert, F., Niederdraenk, F., Barralet, J.E., Gbureck, U., 2009. Ion adsorption behaviour of hydroxyapatite with different crystallinities. Colloids Surf. B Biointerfaces 74 (1), 91–95.
Suetsugu, Y., Takahashi, Y., Okamura, F.P., Tanaka, J., 2000. Structure analysis of A-type carbonate apatite by a single-crystal X-ray diffraction method. J. Solid State Chem. 155 (no. 2), 292–297.
Sugiyama, S., Minami, T., Hayashi, H., Tanaka, M., Moffat, J.B., 1996. Surface and bulk properties of stoichiometric and nonstoichiometric strontium hydroxyapatite and the oxidation of methane. J. Solid State Chem. 126 (2), 242–252.
Sugiyama, S., Minami, T., Higaki, T., Hayashi, H., Moffat, J.B., 1997. High selective conversion of methane to carbon monoxide and the effects of chlorine additives in the gas and solid phases on the oxidation of methane on strontium hydroxyapatites. Ind. Eng. Chem. Res. 36 (2), 328–334.
Sugiyama, S., Iguchi, Y., Nishioka, H., Minami, T., Moriga, T., Hayashi, H., Moffat, J.B., 1998. Effects of the thermal stability and the fine structure changes of strontium hydroxyapatites ion-exchanged with lead on methane oxidation in the presence and absence of tetrachloromethane. J. Catal. 176 (1), 25–34.
Sugiyama, S., Osaka, T., Hirata, Y., Sotowa, K.-I., 2006. Enhancement of the activity for oxidative dehydrogenation of propane on calcium hydroxyapatite substituted with vanadate. Appl. Catal. A Gen. 312, 52–58.
Sun, Y., Qu, Z., Chen, D., Wang, H., Zhang, F., Fu, Q., 2014. Formaldehyde catalytic oxidation over hydroxyapatite modified with various organic molecules. Chin. J. Catal. 35 (12), 1927–1936.
Surmeneva, M.A., Mukhametkaliyev, T.M., Khakbaz, H., Surmenev, R.A., Kannan, M.B., 2015. Ultrathin film coating of hydroxyapatite (HA) on a magnesium–calcium alloy using RF magnetron sputtering for bioimplant applications. Mater. Lett. 152, 280–282.
Surmeneva, M.A., Ivanova, A.A., Tian, Q., Pittman, R., Jiang, W., Lin, J., Liu, H.H., Surmenev, R.A., 2019. Bone marrow derived mesenchymal stem cell response to the RF magnetron sputter deposited hydroxyapatite coating on AZ91 magnesium alloy. Mater. Chem. Phys. 221, 89–98.
Swain, S.K., Sarkar, D., 2013. Study of BSA protein adsorption/release on hydroxyapatite nanoparticles. Appl. Surf. Sci. 286, 99–103.
Tanaka, H., Tsuda, E., Nishikawa, H., Fuji, M., 2012. FTIR studies of adsorption and photocatalytic decomposition under UV irradiation of dimethyl sulfide on calcium hydroxyapatite. Adv. Powder Technol. 23 (1), 115–119.
Tibbetts, C., Johansson, K., Philipson, L., 1973. Hydroxyapatite chromatography and formamide denaturation of adenovirus DNA. J. Virol. 12 (2), 218–225.
Tiselius, A., Hjerten, S., Levin, Ö., 1956. Protein chromatography on calcium phosphate columns. Arch. Biochem. Biophys. 65 (1), 132–155.
Tounsi, H., Djemal, S., Petitto, C., Delahay, G., 2011. Copper loaded hydroxyapatite catalyst for selective catalytic reduction of nitric oxide with ammonia. Appl. Catal. B Environ. 107 (1), 158–163.
Trombe, J.C., Montel, G., 1978. Some features of the incorporation of oxygen in different oxidation states in the apatitic lattice—I on the existence of calcium and strontium oxyapatites. J. Inorg. Nucl. Chem. 40 (1), 15–21.
Tsuchida, T., Kubo, J., Yoshioka, T., Sakuma, S., Takeguchi, T., Ueda, W., 2008. Reaction of ethanol over hydroxyapatite affected by Ca/P ratio of catalyst. J. Catal. 259 (2), 183–189.
Ungureanu, D.N., Angelescu, N., Bacinschi, Z., Stoian, E.V., Rizescu, C.Z., 2011. Thermal stability of chemically precipitated hydroxyapatite nanopowders. Int. J. Biol. Biomed. Eng. 5 (2), 57–64.
Veiderma, M., Tõnsuaadu, K., Knubovets, R., Peld, M., 2005. Impact of anionic substitutions on apatite structure and properties. J. Organomet. Chem. 690 (10), 2638–2643.
Venugopal, A., Scurrell, M.S., 2003. Hydroxyapatite as a novel support for gold and ruthenium catalysts: behaviour in the water gas shift reaction. Appl. Catal. A Gen. 245 (1), 137–147.
Veselinović, L., Karanović, L., Stojanović, Z., Bračko, I., Marković, S., Ignjatović, N., Uskoković, D., 2010. Crystal structure of cobalt-substituted calcium hydroxyapatite nanopowders prepared by hydrothermal processing. J. Appl. Crystallogr. 43 (2), 320–327.
Vila, M., Sánchez-Salcedo, S., Cicuéndez, M., Izquierdo-Barba, I., Vallet-Regí, M., 2011. Novel biopolymer-coated hydroxyapatite foams for removing heavy-metals from polluted water. J. Hazard. Mater. 192 (1), 71–77.
Wakamura, M., Kandori, K., Ishikawa, T., 2000. Surface structure and composition of calcium hydroxyapatites substituted with Al (III), La (III) and Fe (III) ions. Colloids Surf. Physicochem. Eng. Asp. 164 (2), 297–305.
Wakamura, M., Tanaka, H., Naganuma, Y., Yoshida, N., Watanabe, T., 2011. Surface structure and visible light photocatalytic activity of titanium–calcium hydroxyapatite modified with Cr (III). Adv. Powder Technol. 22 (4), 498–503.
Wang, Y., Zhang, S., Zeng, X., Ma, L.L., Weng, W., Yan, W., Qian, M., 2007. Osteoblastic cell response on fluoridated hydroxyapatite coatings. Acta Biomater. 3 (2), 191–197.
Wang, J.-D., Liu, J.-K., Lu, Y., Hong, D.-J., Yang, X.-H., 2014. Catalytic performance of gold nanoparticles using different crystallinity hap as carrier materials. Mater. Res. Bull. 55, 190–197.
Wang, Y., Chen, B., Crocker, M., Zhang, Y., Zhu, X., Shi, C., 2015. Understanding on the origins of hydroxyapatite stabilized gold nanoparticles as high-efficiency catalysts for formaldehyde and benzene oxidation. Catal. Commun. 59, 195–200.
Wang, H., Wang, C., Xiao, B., Zhao, L., Zhang, J., Zhu, Y., Guo, X., 2016. The hydroxyapatite nanotube as a promoter to optimize the HDS reaction of NiMo/TiO_2 catalyst. Catal. Today 259 (Part 2), 340–346.
Watanabe, T., Makitsuru, K., Nakazawa, H., Hara, S., Suehiro, T., Yamamoto, A., Hiraide, T., Ogawa, T., 1999. Separation of double-strand DNA fragments by high-performance liquid chromatography using a ceramic hydroxyapatite column. Anal. Chim. Acta 386 (1–2), 69–75.
Weerasuriya, D.R.K., Wijesinghe, W., Rajapakse, R.M.G., 2017. Encapsulation of anticancer drug copper bis (8-hydroxyquinoline) in hydroxyapatite for pH-sensitive targeted delivery and slow release. Mater. Sci. Eng. C 71, 206–213.
Wei, W., Sun, R., Cui, J., Wei, Z., 2010. Removal of nitrobenzene from aqueous solution by adsorption on nanocrystalline hydroxyapatite. Desalination 263 (1–3), 89–96.
Wei, W., Yang, L., Zhong, W., Cui, J., Wei, Z., 2015. Poorly crystalline hydroxyapatite: a novel adsorbent for enhanced fulvic acid removal from aqueous solution. Appl. Surf. Sci. 332, 328–339.
Wlóka, D., Placek, A., Smol, M., Rorat, A., Hutchison, D., Kacprzak, M., 2019. The efficiency and economic aspects of phytoremediation technology using Phalaris arundinacea L. and Brassica napus L. combined with compost and nano SiO_2 fertilization for the removal of PAH's from soil. J. Environ. Manage. 234, 311–319.
Wu, H., Yan, H., Quan, Y., Zhao, H., Jiang, N., Yin, C., 2018. Recent progress and perspectives in biotrickling filters for VOCs and odorous gases treatment. J. Environ. Manage. 222, 409–419.
Xie, J., Meng, X., Zhou, Z., Li, P., Yao, L., Bian, L., Gao, X., Wei, Y., 2013. Preparation of titania/hydroxyapatite (TiO_2/HAp) composite photocatalyst with mosaic structure for degradation of pentachlorophenol. Mater. Lett. 110, 57–60.
Xu, Y., Schwartz, F.W., Traina, S.J., 1994. Sorption of Zn^{2+} and Cd^{2+} on hydroxyapatite surfaces. Environ. Sci. Technol. 28 (8), 1472–1480.
Xu, J., White, T., Li, P., He, C., Han, Y.-F., 2010. Hydroxyapatite foam as a catalyst for formaldehyde combustion at room temperature. J. Am. Chem. Soc. 132 (38), 13172–13173.
Yan, B., Zhang, Y., Chen, G., Shan, R., Ma, W., Liu, C., 2016. The utilization of hydroxyapatite-supported CaO-CeO_2 catalyst for biodiesel production. Energy Convers. Manage. 130, 156–164.
Yao, J., Zhang, Y., Wang, Y., Chen, M., Huang, Y., Cao, J., Ho, W., Cheng Lee, S., 2017. Enhanced photocatalytic removal of NO over titania/hydroxyapatite (TiO_2/HAp) composites with improved adsorption and charge mobility ability. RSC Adv. 7 (40), 24683–24689.
Yin, G., Liu, Z., Zhan, J., Ding, F., Yuan, N., 2002. Impacts of the surface charge property on protein adsorption on hydroxyapatite. Chem. Eng. J. 87 (2), 181–186.
Yoruç, A.H., Karakaş, A., Koyun, A., Yildiz, T., 2012. Comparison of properties of hydroxyapatite powders synthesized by chemical and biomimetic techniques. Acta Phys. Pol. A 121 (1), 233–235.
Zhang, S., 2013. Hydroxyapatite Coatings for Biomedical Applications. CRC Press.
Zhang, S., Xianting, Z., Yongsheng, W., Kui, C., Wenjian, W., 2006. Adhesion strength of sol–gel derived fluoridated hydroxyapatite coatings. Surf. Coat. Technol. 200 (22–23), 6350–6354.
Zhao, K., Qiao, B., Wang, J., Zhang, Y., Zhang, T., 2011. A highly active and sintering-resistant Au/FeO_x–hydroxyapatite catalyst for CO oxidation. Chem. Commun. 47 (6), 1779–1781.
Zhao, K., Qiao, B., Zhang, Y., Wang, J., 2013. The roles of hydroxyapatite and FeO_x in a Au/FeO_x hydroxyapatite catalyst for CO oxidation. Chin. J. Catal. 34 (7), 1386–1394.
Zhou, Y., Chang, D., Chang, J., 2017. Preparation of nano-structured pig bone hydroxyapatite for high-efficiency adsorption of Pb^{2+} from aqueous solution. Int. J. Appl. Ceram. Technol. 14 (6), 1125–1133.
Zhu, K., Yanagisawa, K., Shimanouchi, R., Onda, A., Kajiyoshi, K., 2006. Preferential occupancy of metal ions in the hydroxyapatite solid solutions synthesized by hydrothermal method. J. Eur. Ceram. Soc. 26 (4), 509–513.
Zhuang, Z., Aizawa, M., 2013. Protein adsorption on single-crystal hydroxyapatite particles with preferred orientation to a (b)-and c-axes. J. Mater. Sci. Mater. Med. 24 (5), 1211–1216.
Zilm, M., Thomson, S.D., Wei, M., 2015. A comparative study of the sintering behavior of pure and manganese-substituted hydroxyapatite. Materials 8 (9), 6419–6436.